GREAT DESIGNS IN STEEL

EVALUATION OF DAMAGE ACCUMULATION FRACTURE MODELS IN NON-LINEAR STRAIN PATHS

Prof. Cliff Butcher

University of Waterloo

2023

PROJECT TEAM

University of Waterloo
Armin Abedini, PhD, Project manager
Farinaz Khameneh, PhD Candidate
Jacqueline Noder, PhD
Cole Fast-Irvine, MASc
Kenneth Cheong, PhD Student
Cliff Butcher, Associate Professor

Auto-Steel Partnership: Constitutive & Fracture Modelling Team
Eric McCarty, A/SP Project Manager

<u>Technical Leads for DP1180 Project</u>
Dr. Thomas Stoughton, General Motors
Dr. Andrey Ilinich, Ford Motor Company

OVERVIEW OF FRACTURE MODELLING FOR CRASH

1. Construct Proportional Fracture Loci from Coupon Tests:
Experimental or Inverse FE Approaches Used

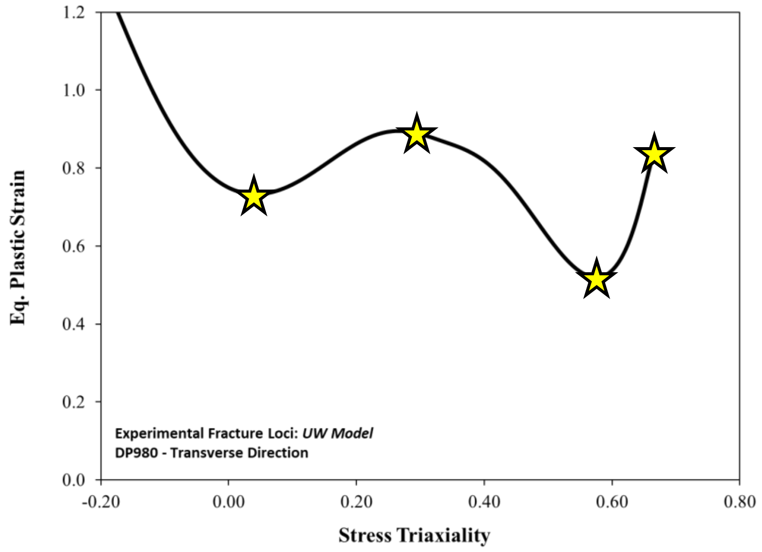

Step 2. Assume Damage Model for
Non-Linear Loading. Pair with Fracture Locus

$$\Delta D^{GISSMO} = \left[\frac{n}{\varepsilon_f^{\exp}(T)} D^{\left(1-\frac{1}{n}\right)}\right]\Delta\varepsilon^{p}$$

Step 3. Regularize for element size
& apply to structural CAE models

Need Objective Evaluation of
Phenomenological Fracture Models

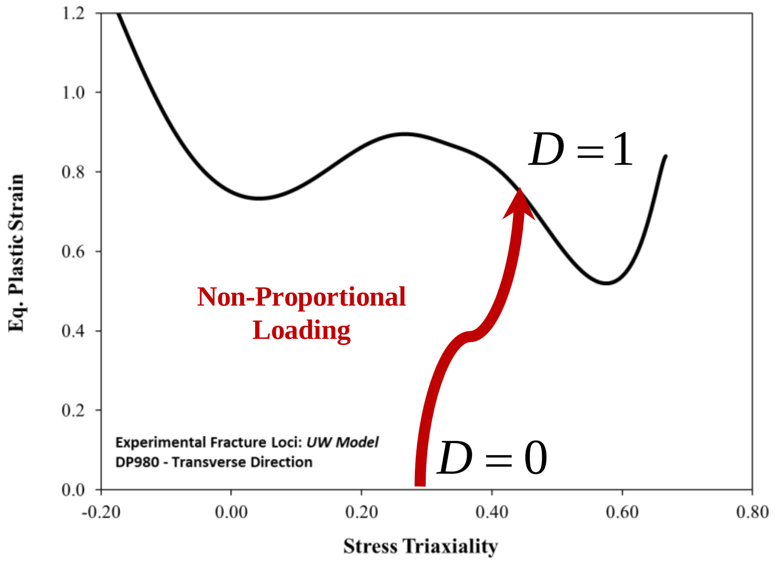

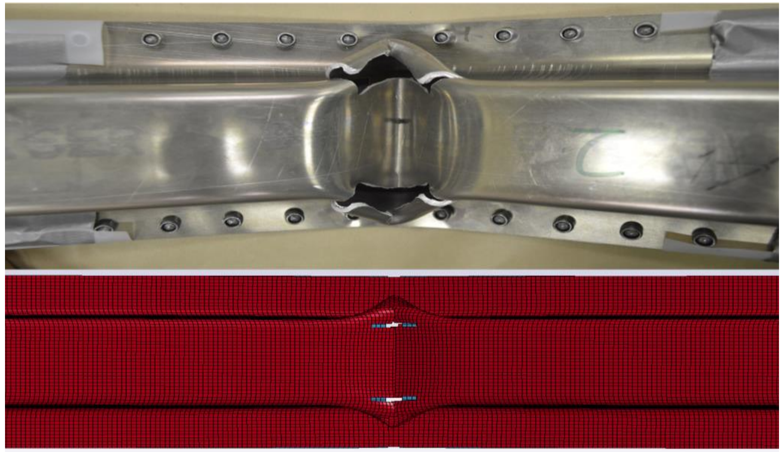

3-Point Bend of Rail Section

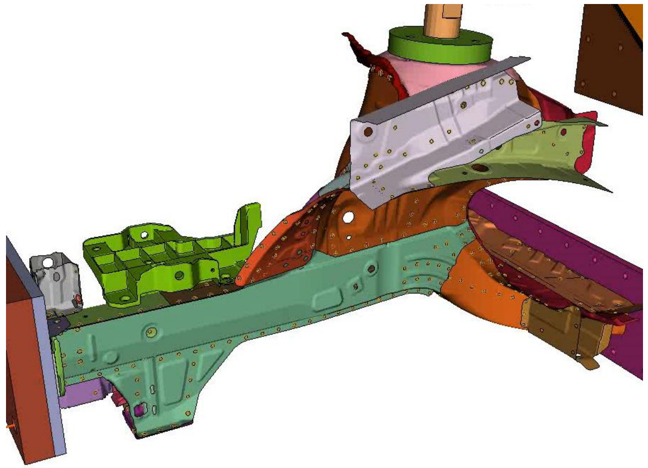

Axial Crush of Front End Crush Structure

Axial Crush of Hot Stamped Rail

BRIEF REVIEW OF PROPORTIONAL FRACTURE

Example: Consider isotropically hardening material. Yield surface expands

Fracture: Define failure surface: Tresca is simplest with straight line for fracture

Intersection of yield and fracture surface creates the fracture locus (2D) or surface (3D)

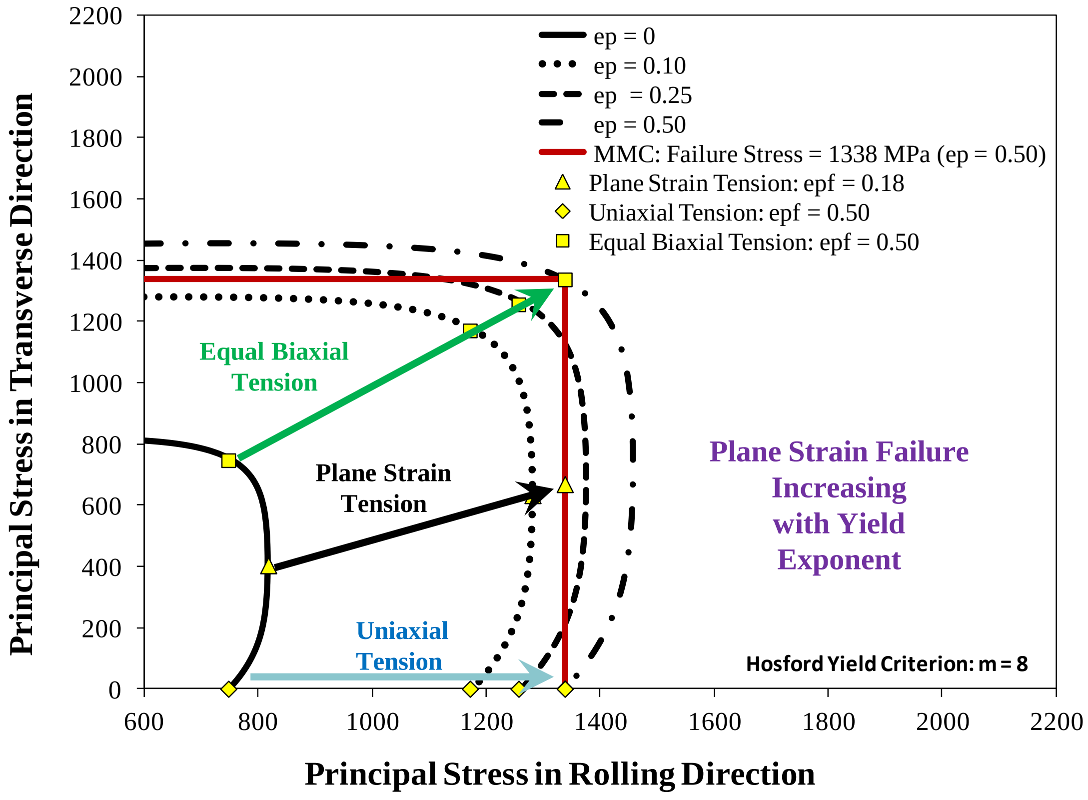

$$\boxed{(\sigma_1)^f = \text{constant (plane stress, tensile quadrant)}}$$

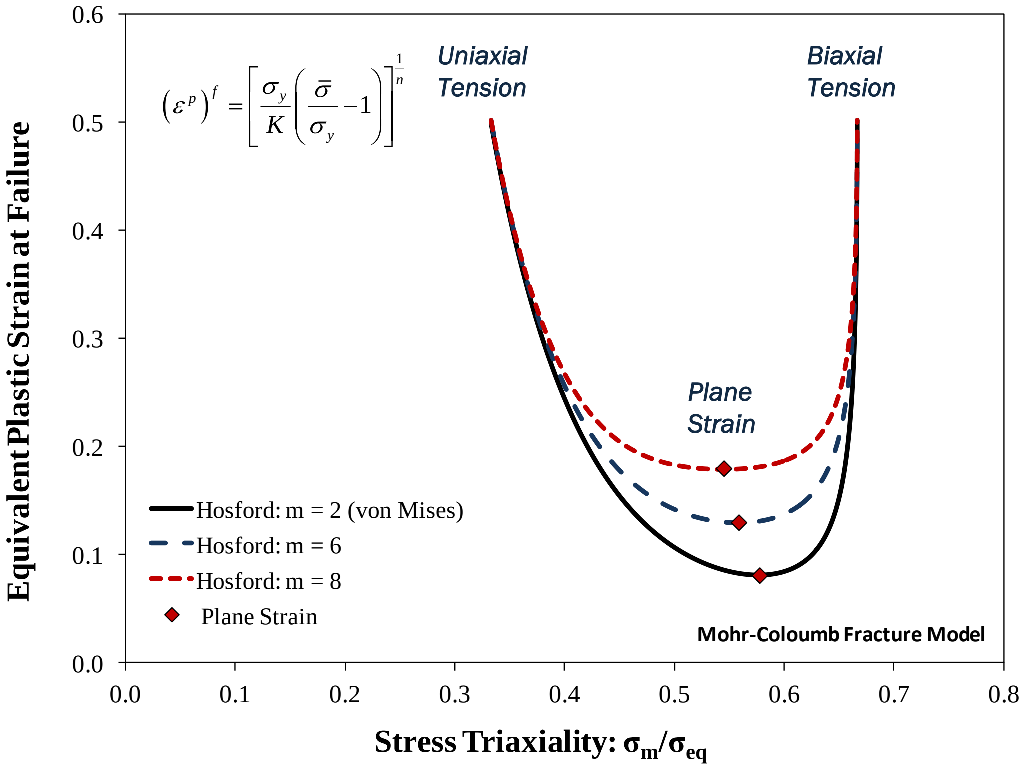

Plane Strain Valley: Depends on hardening and yield surface

BRIEF REVIEW OF PROPORTIONAL FRACTURE

Change Tresca to Mohr-Coloumb for Difference in Tension and Compression (still linear fracture model)

Mohr-Coulomb Criterion: $$\sigma_1 - \sigma_3 + c(\sigma_1 + \sigma_3) = b$$

b = related to shear stress;

c = cohesion (controls compressive response)
c = 0 (Tresca – Max shear stress criterion)

C parameter acts as hinge at uniaxial tension. Cusp in plane stress fracture locus created by corner

Problem Statement: Identify the Fracture Potential Function in Stress Space. Natural extension to anisotropy, complex loading

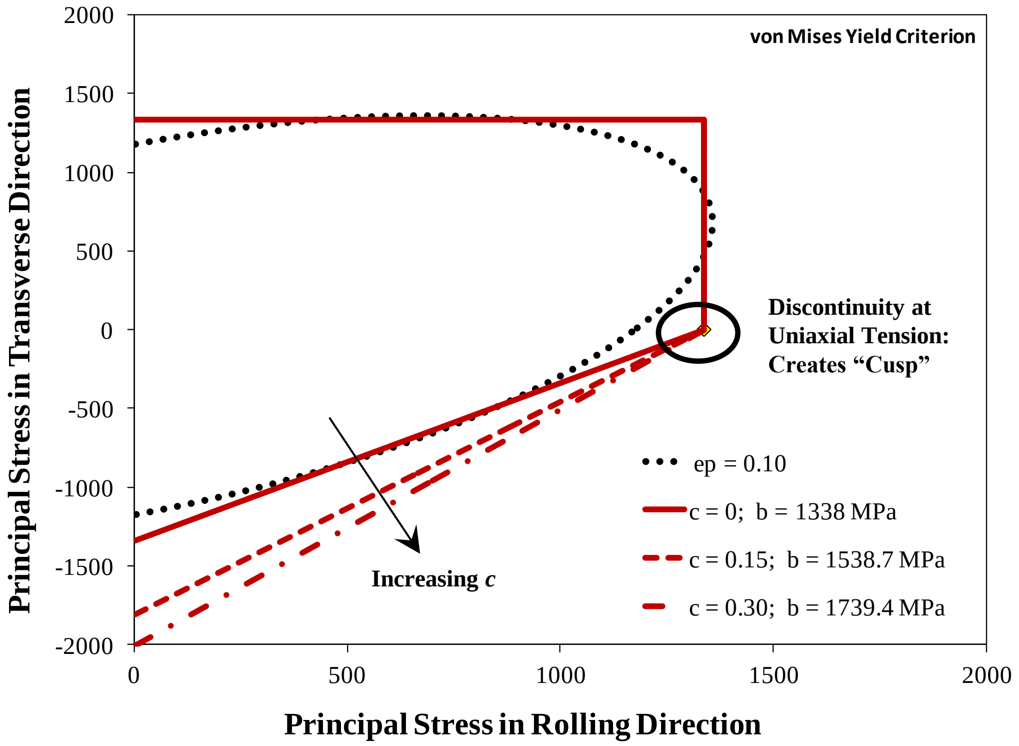

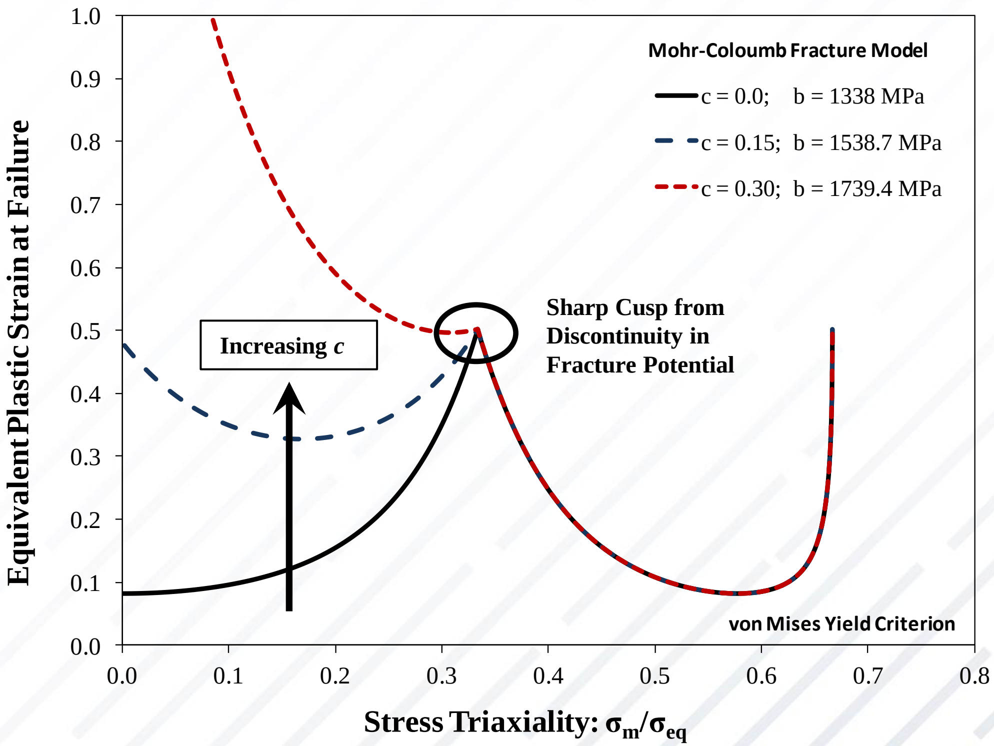

BRIEF REVIEW OF PROPORTIONAL FRACTURE

Inversion of fracture surface with yield and hardening models used to create equivalent strain representation with triaxiality and Lode parameter. Ex: MMC-5 parameter model

$$\varepsilon_f^{MMC5} = \left[c_2 \left[c_\theta^s + \frac{\sqrt{3}}{2-\sqrt{3}} \left(c_\theta^{ax} - c_\theta^s \right) \left(\sec\left(\frac{\pi\bar{\theta}}{6} \right) - 1 \right) \right] \left(\frac{\sqrt{3}}{3} \cos\left(\frac{\pi\bar{\theta}}{6} \right) + c_1 \left[T + \frac{1}{3} \sin\left(\frac{\pi\bar{\theta}}{6} \right) \right] \right) \right]^{\frac{-1}{c_n}} \qquad T = \frac{\sigma_{\text{hyd}}}{\sigma_{eq}^{\text{von Mises}}} \qquad \bar{\theta} = 1 - \frac{2}{\pi} \cos^{-1}\left(\frac{27}{2} \frac{J_3}{\left(\sigma_{eq}^{\text{vM}} \right)^3} \right)$$

Convenient but breaks explicit link between plasticity and fracture surface. Now many versions in the literature

<u>Procedure for Experimental Fracture Characterization</u>

1. *Characterize plasticity and hardening behavior*
2. *Characterize fracture strains in proportional loading*
   → what tests to use?
3. *Select & calibrate fracture function*
   → Shape can vary between calibration points…
4. *How to generalize to non-proportional model*
   → need damage model if using eq. strain (ex: GISSMO)

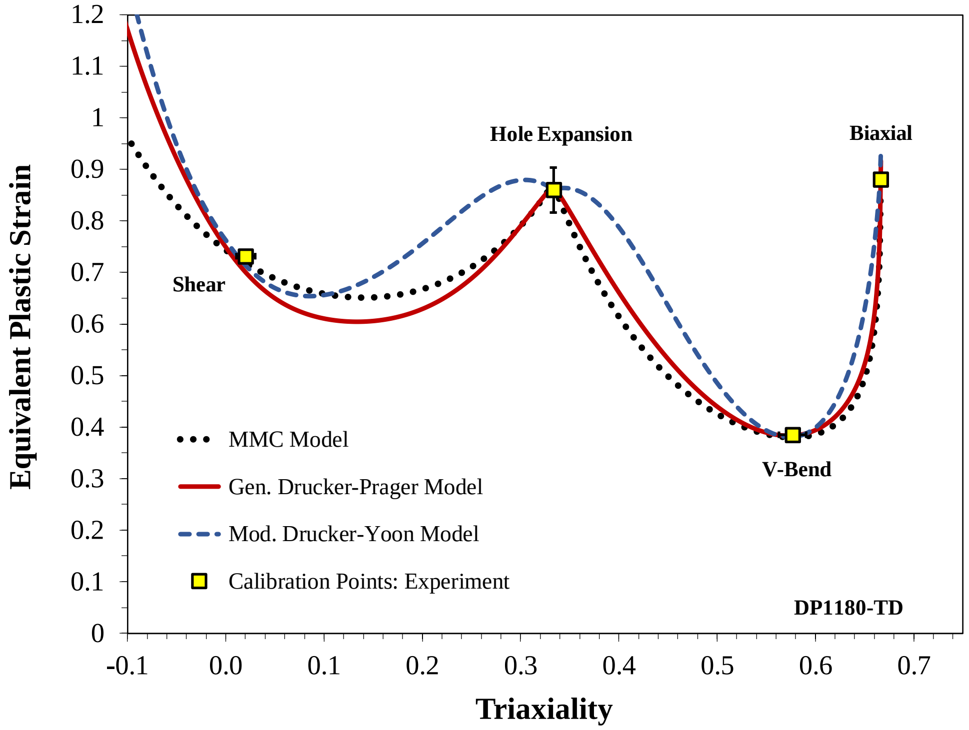

ANISOTROPIC PLASTICITY

Detailed experimental characterization of anisotropy:

- Uniaxial tension (7 directions)
- Simple shear (3 directions)
- Plane Strain tension (3 directions)
- Disc compression test for biaxial R-value

Non-associated Yld2018 (Drucker-type) yield & plastic potential

Yld2018 Yield Function	$c_1^{(1)}$	$c_2^{(1)}$	$c_3^{(1)}$	$c_6^{(1)}$
	1.6080	1.2208	-1.2501	-0.1263
	$c_1^{(2)}$	$c_2^{(2)}$	$c_3^{(2)}$	$c_6^{(2)}$
	1.8253	2.2858	0.9587	2.2471
	$c_1^{(3)}$	$c_2^{(3)}$	$c_3^{(3)}$	$c_6^{(3)}$
	1.8204	1.8062	3.8849	2.5860
Yld2018 Plastic Potential	$c_1^{(1)}$	$c_2^{(1)}$	$c_3^{(1)}$	$c_6^{(1)}$
	-1.4247	-1.1807	-2.5197	-1.7997
	$c_1^{(2)}$	$c_2^{(2)}$	$c_3^{(2)}$	$c_6^{(2)}$
	-2.3117	-3.4206	-2.1952	-2.7765
	$c_1^{(3)}$	$c_2^{(3)}$	$c_3^{(3)}$	$c_6^{(3)}$
	-1.4638	-0.7428	-0.4724	-0.7330

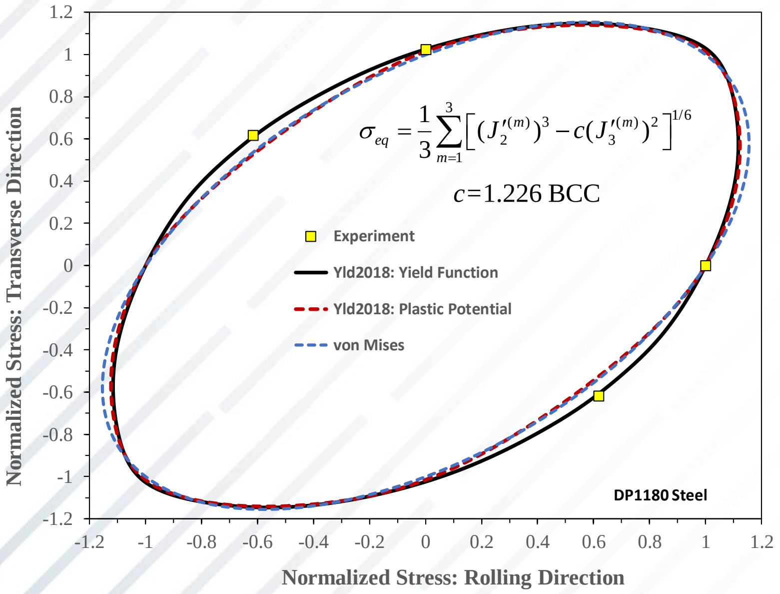

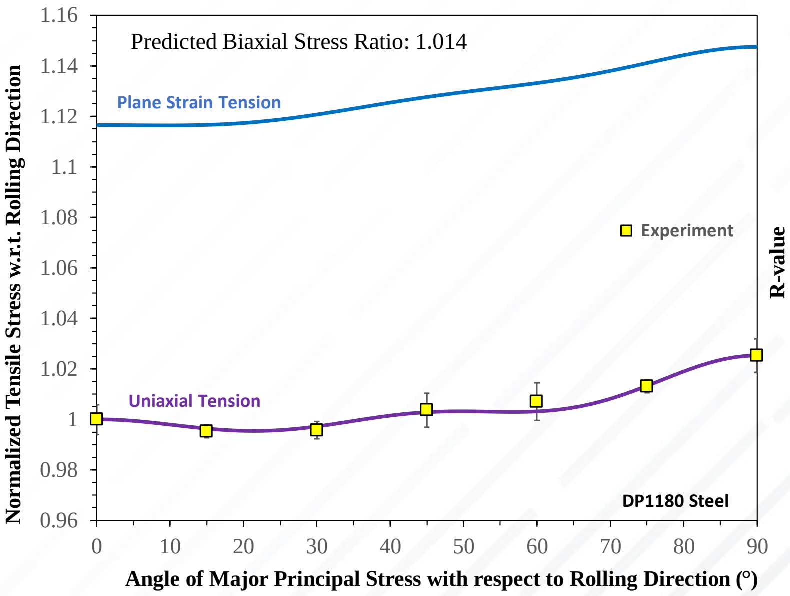

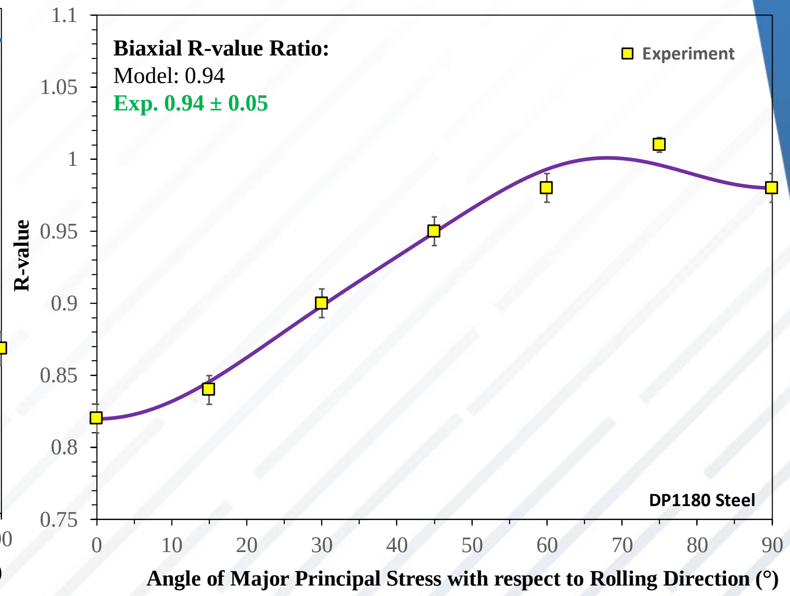

CONSTITUTIVE CHARACTERIZATION

Shear hardening behavior nearly identical in RD-TD and TD-RD shear loading (orthotropic yield surface)

→ Reverse shear test did not show complex hardening response. Reversion to monotonic shear response

→ Characterization of hardening in complex strain path changes outside of scope → future work

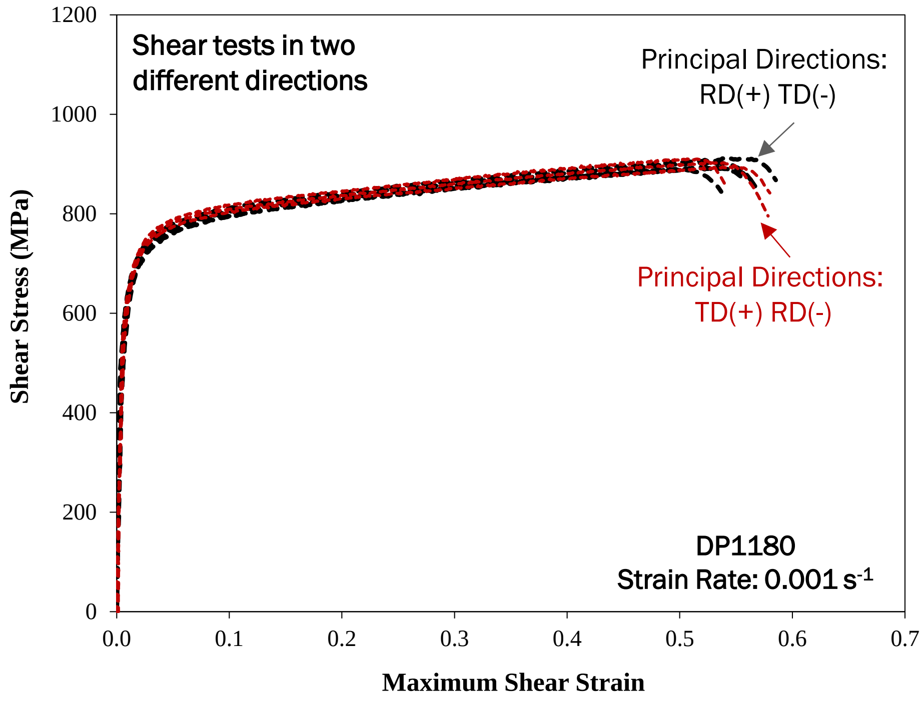

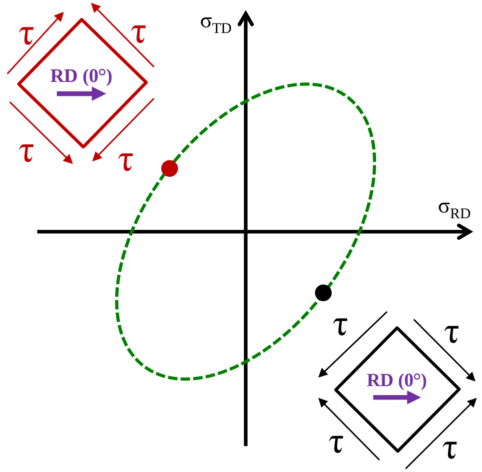

Assumption of orthotropic response is typical in popular yield criteria like Yld2000, Yld2004, Yoshida, e

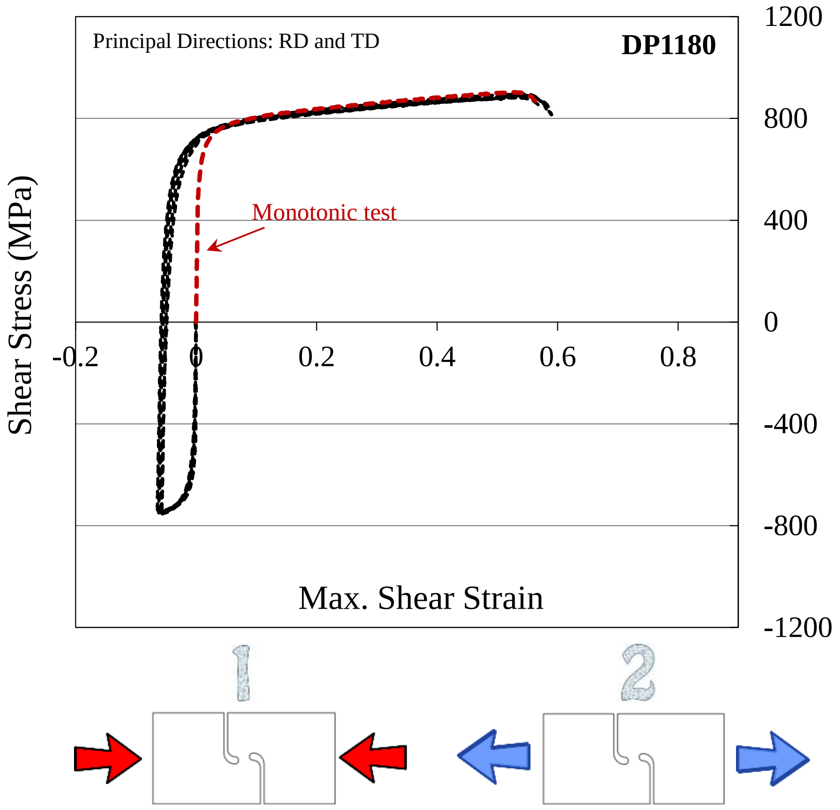

ISOTROPIC HARDENING BEHAVIOR

Hardening to large strains obtained using UW's shear conversion methodology in RD & TD

→ Uniform elongation is ~5% but shear conversion provides data to 60% plastic strain

→ Isotropic hardening reasonable assumption for DP1180

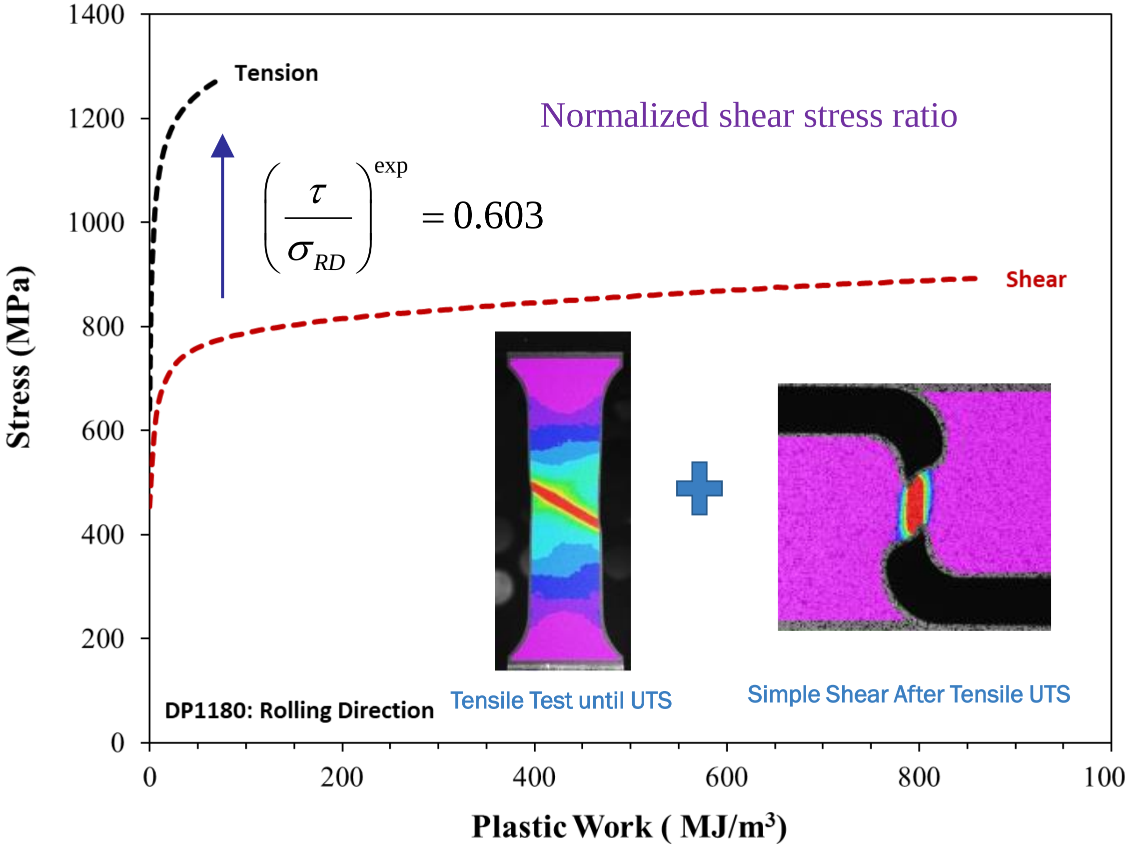

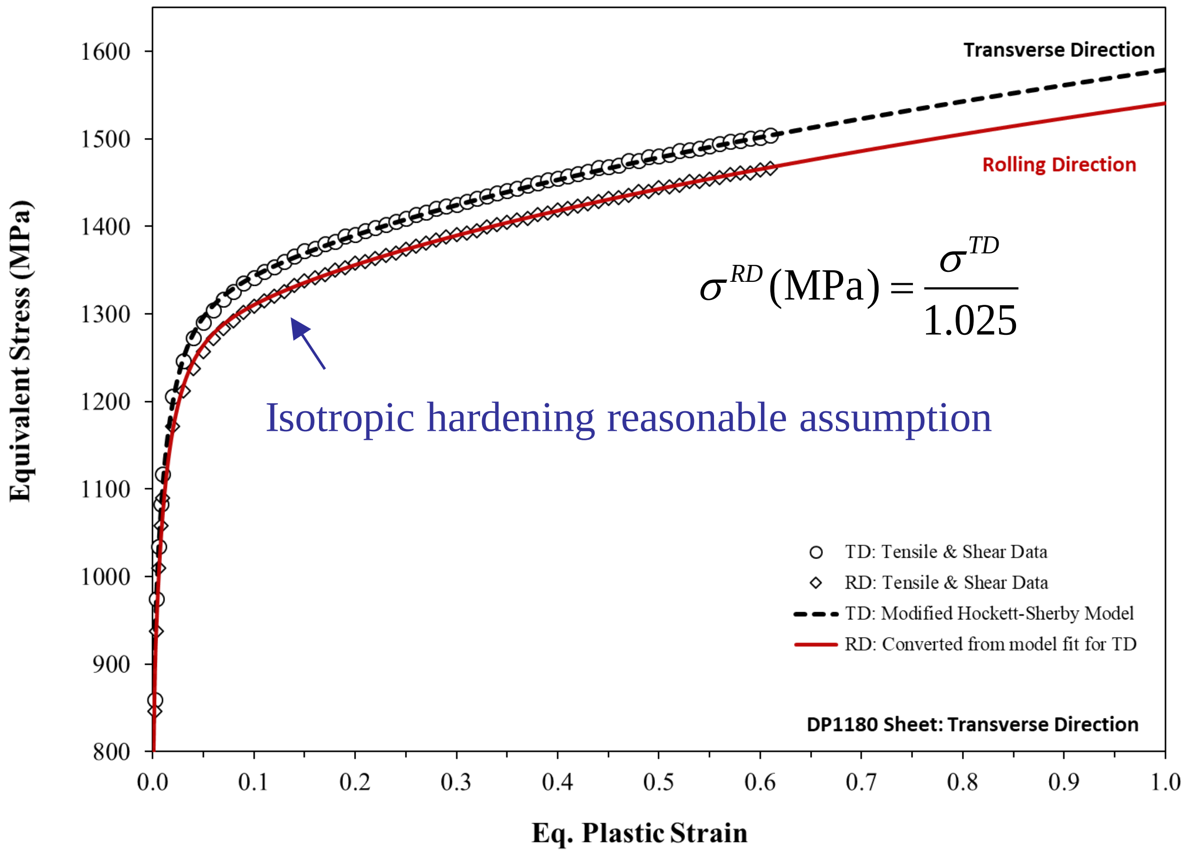

Abedini A, Noder J, Kohar C, Butcher C, *Mechanics of Materials*, 2020, 148:103419

EVALUATIONS OF PLASTICITY MODEL

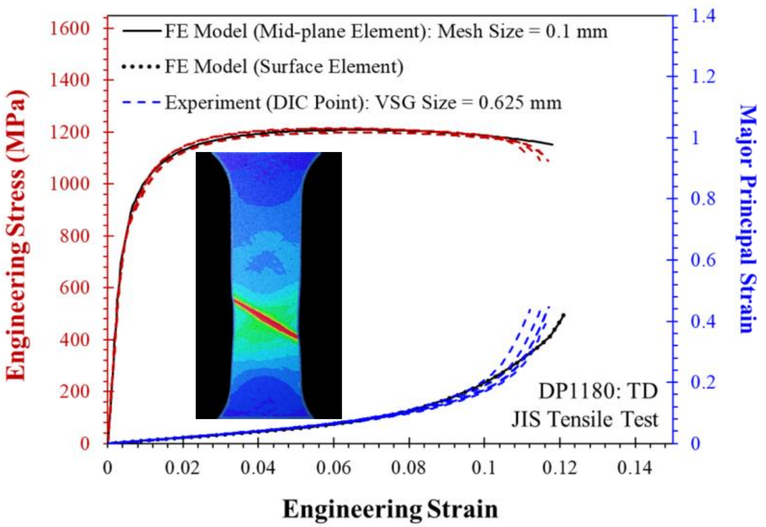

JIS Tensile (shear band)

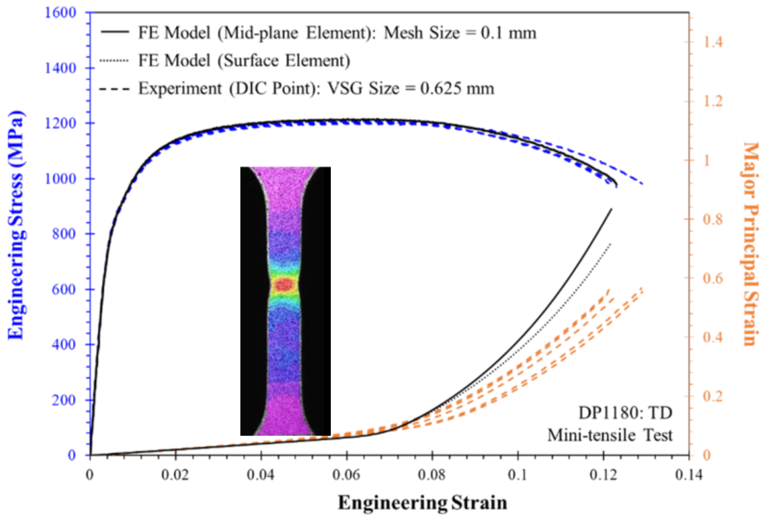

Mini Tensile (triaxial neck)

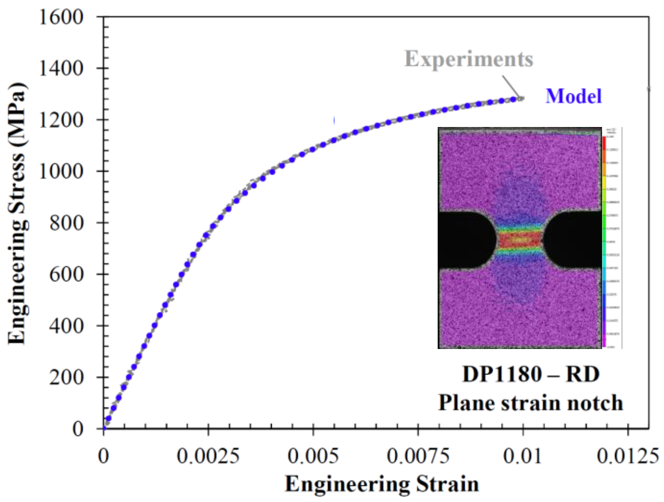

Plane Strain Notch Tension

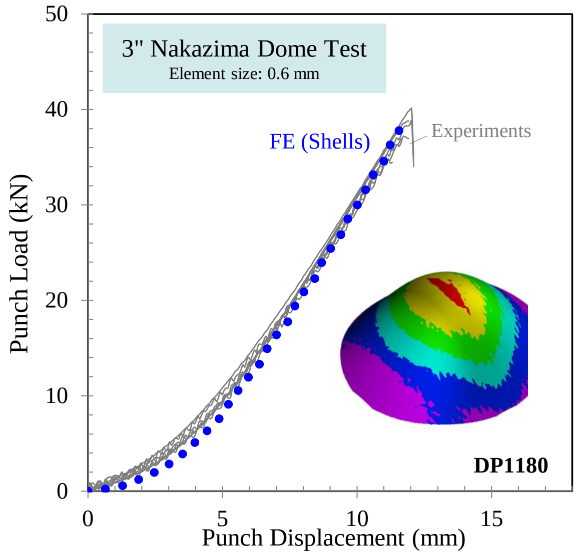

Nakazima Dome Test

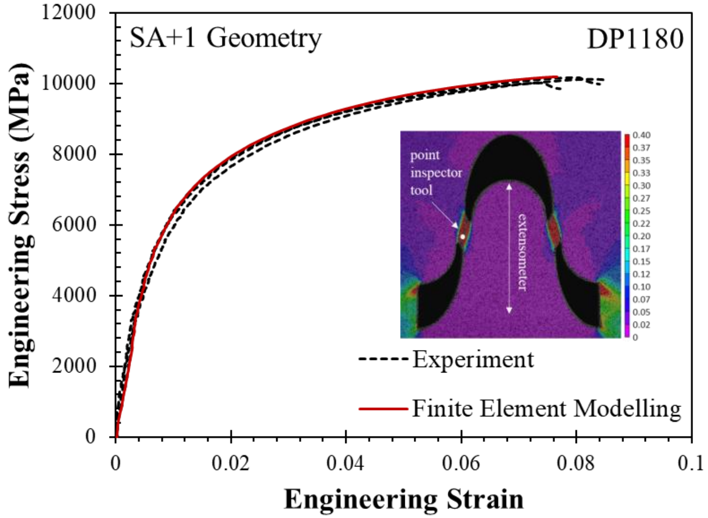

Combined Tension & Shear

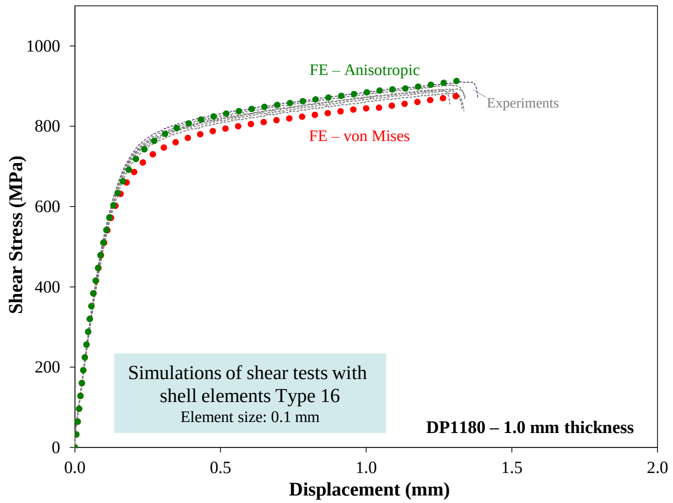

Simple Shear

FORMABILITY IN TRANSVERSE DIRECTION

Forming limit curve (FLC) required to identify pre-straining limits for fracture tests

Marciniak and Nakazima tests performed in Transverse direction (limiting direction)

→ Process corrections for Nakazima converged to Marciniak limit strains

→ Modified Maximum Force Criterion (MMFC) predicted the FLC. No calibration parameters!

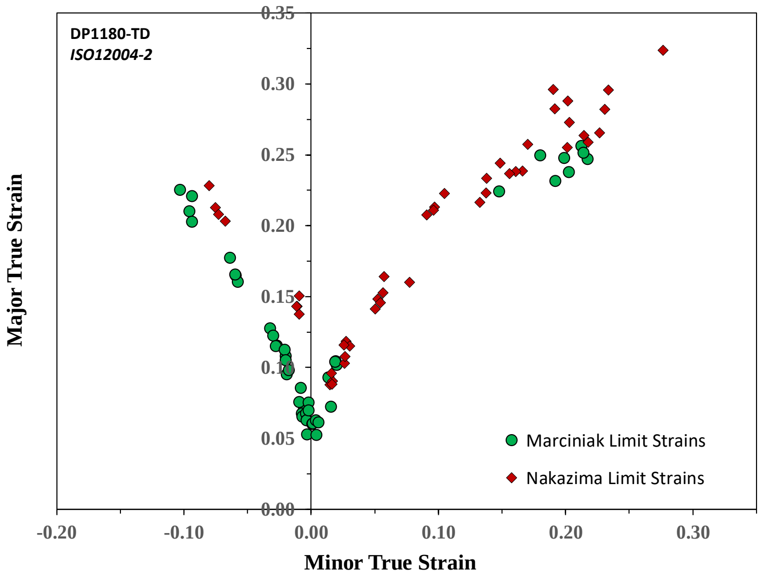

Marciniak & Nakazima Limit Strains

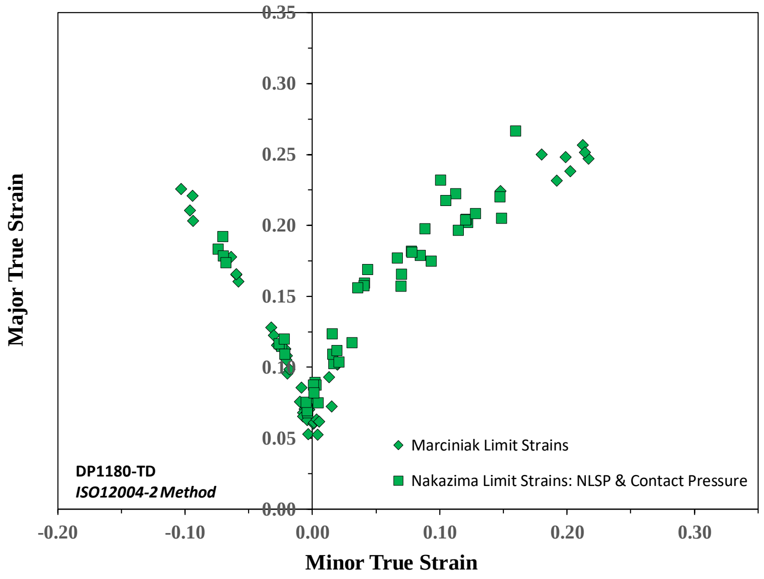

Marciniak & Corrected Nakazima Limit Strains

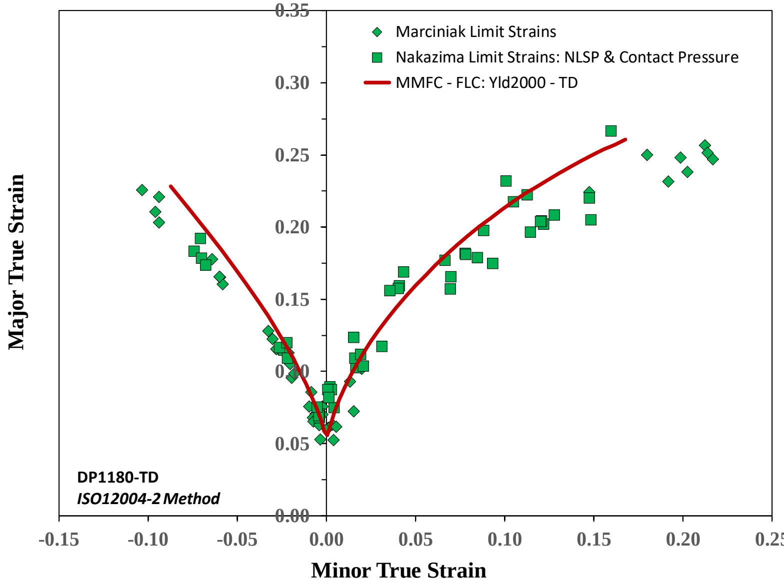

Comparison with Predicted FLC

Butcher et al. (2021). Journal of Materials Processing Technology. 287, 1-18

Min, J., Stoughton, T. B., Carsley, J. E., Lin, J. (2016). International Journal of Mechanical Sciences, 117, 115-134.

Hora P, Tong L, Reissner J, Modified maximum force criterion, a model for theoretical prediction of forming limit curves, *Int J Mater Form*, 2013, 6:267-279.

PROPORTIONAL FRACTURE: SIMPLE SHEAR

Shear fracture strains extremely sensitive to DIC settings and gage length

Detailed study in Khameneh et al. (2022)

→ Used DIC gage length of 0.50 mm throughout the study

→ Fracture *appeared* to occur in center of gauge region based on void damage

Void formation in Mini-shear prior to Fracture

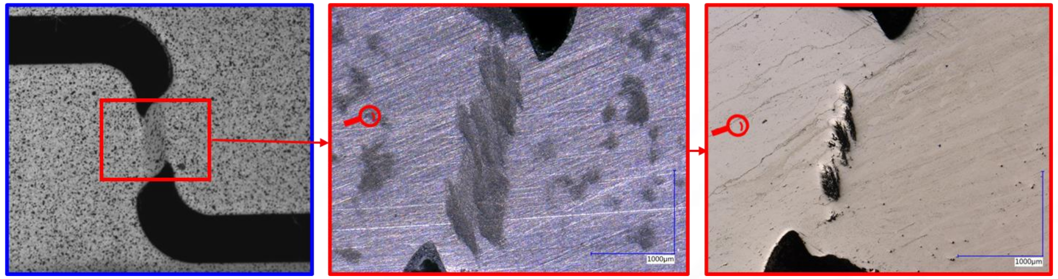

Void formation in Combined Tension & Shear Test: *Average Triaxiality ~ 0.20*

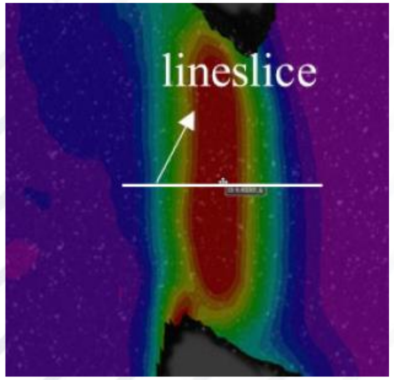

Shear strain can be measured from DIC & line rotation

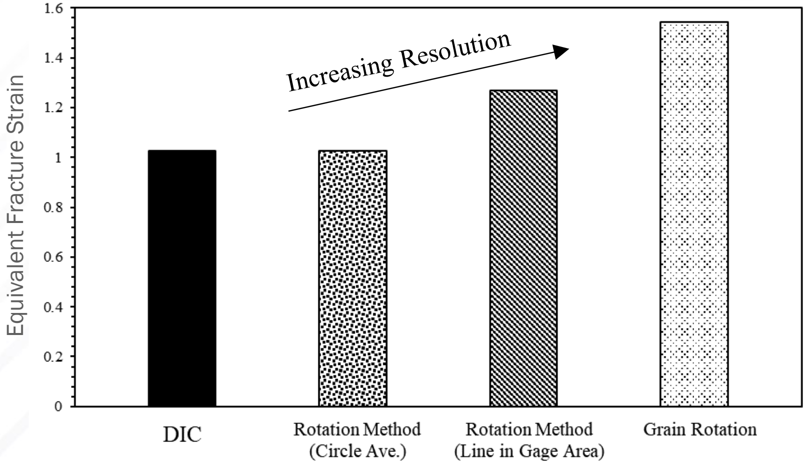

Strong sensitivity to gage length

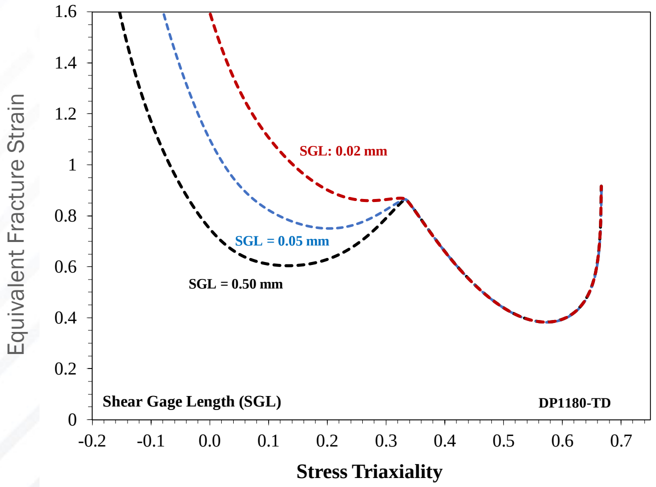

Influence of gage length on fracture locus

PROPORTIONAL FRACTURE: PLANE STRAIN

V-bend test (VDA238-100) most reliable for plane strain fracture characterization

→ V-bend provides proportional plane strain tension without necking

→ DIC is inaccurate for Plane strain tests with necking. Stress state is triaxial…

→ Necking-based tests can be improved with thickness strain correction

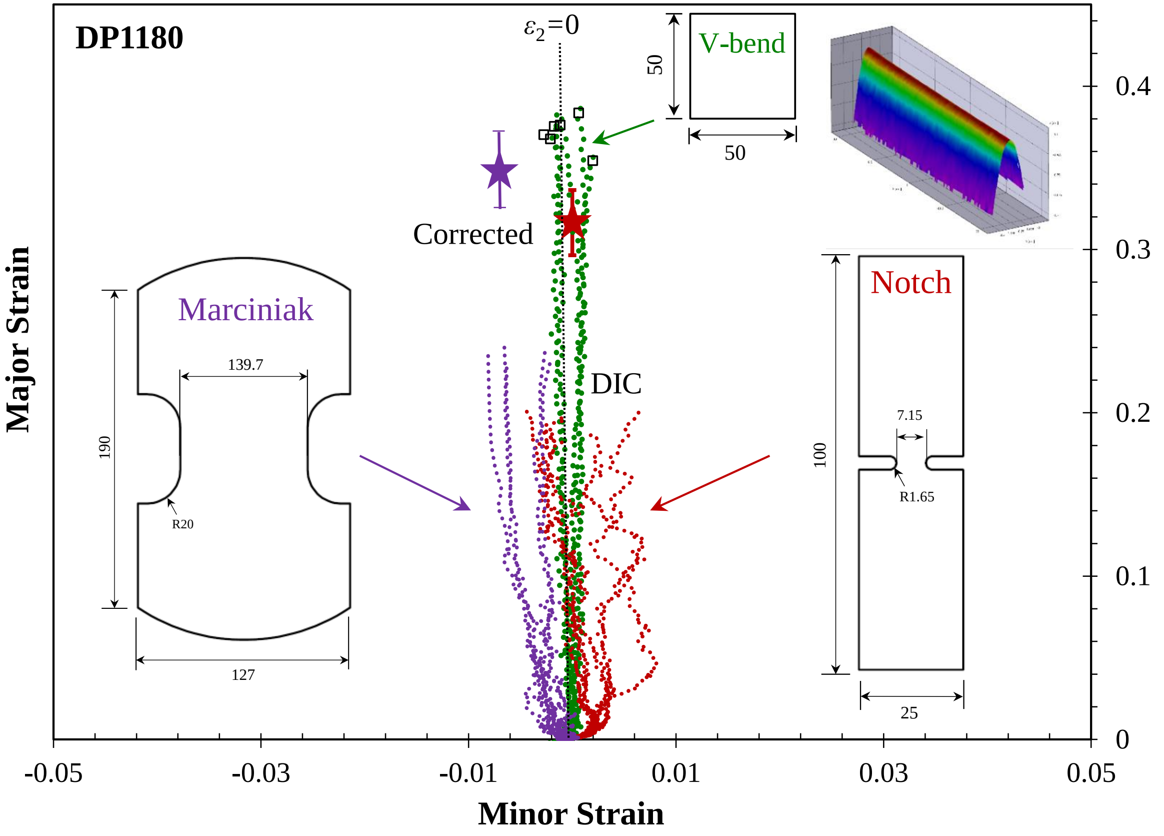

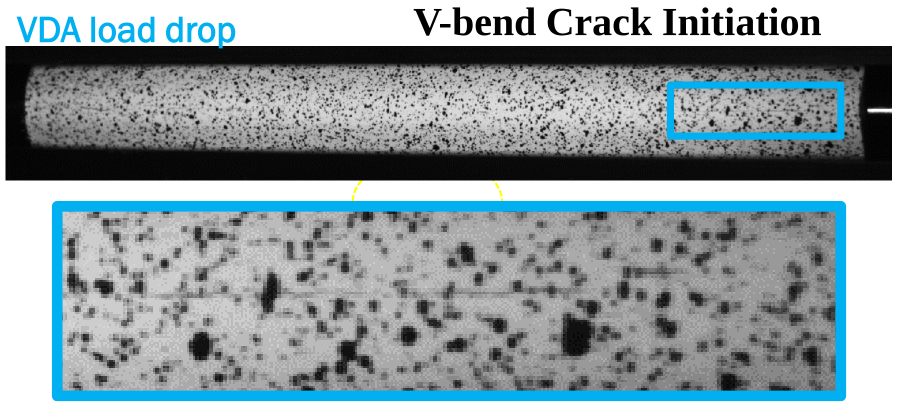

Fracture Strain at VDA load threshold

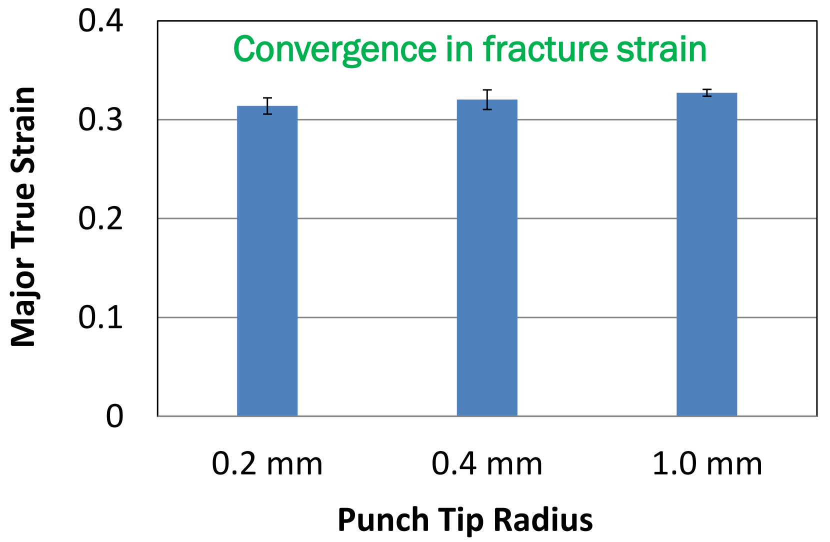

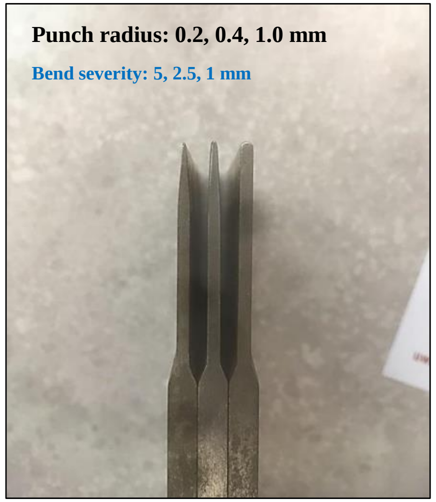

PROPORTIONAL FRACTURE: BIAXIAL STRETCHING

Biaxial fracture strains are significantly affected by necking

→ Smaller punch radii suppress necking and create linear strain path to much higher strains

→ Apparent linearity can be misleading. Incremental analysis shows localization

→ Nakazima (R = 50 mm), Marciniak and Bulge tests tend to be lower bounds for biaxial strains in AHSS

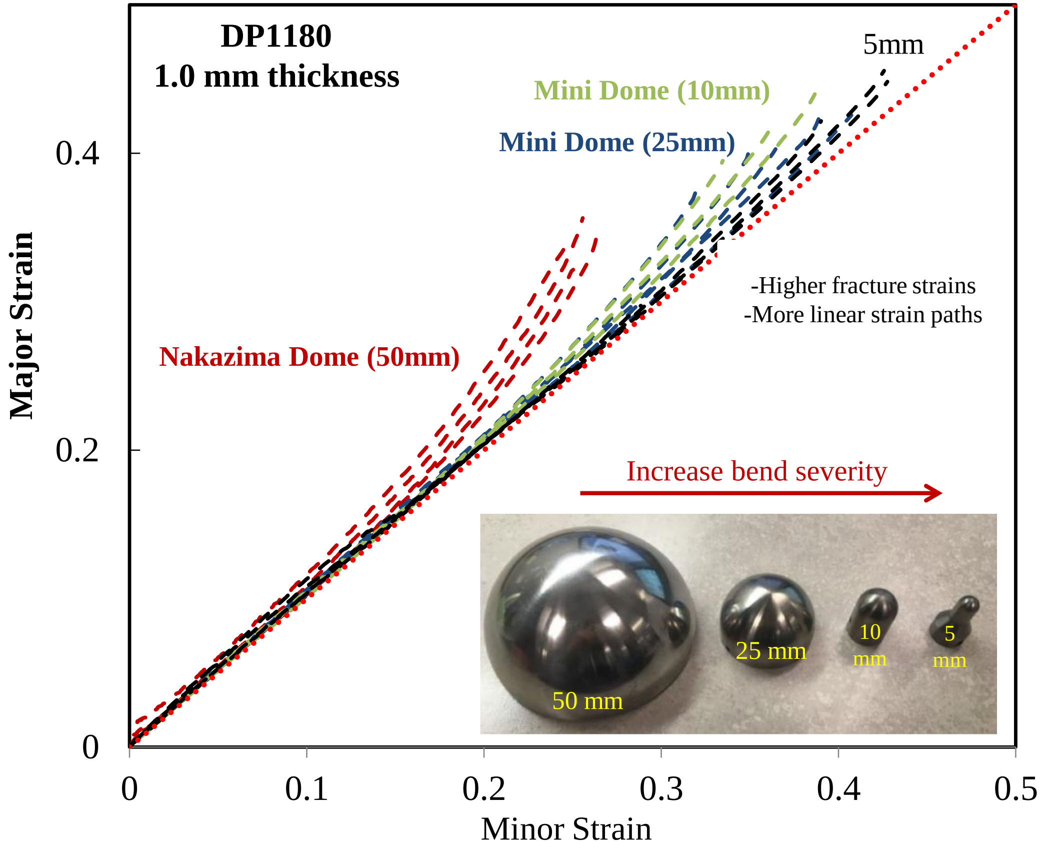

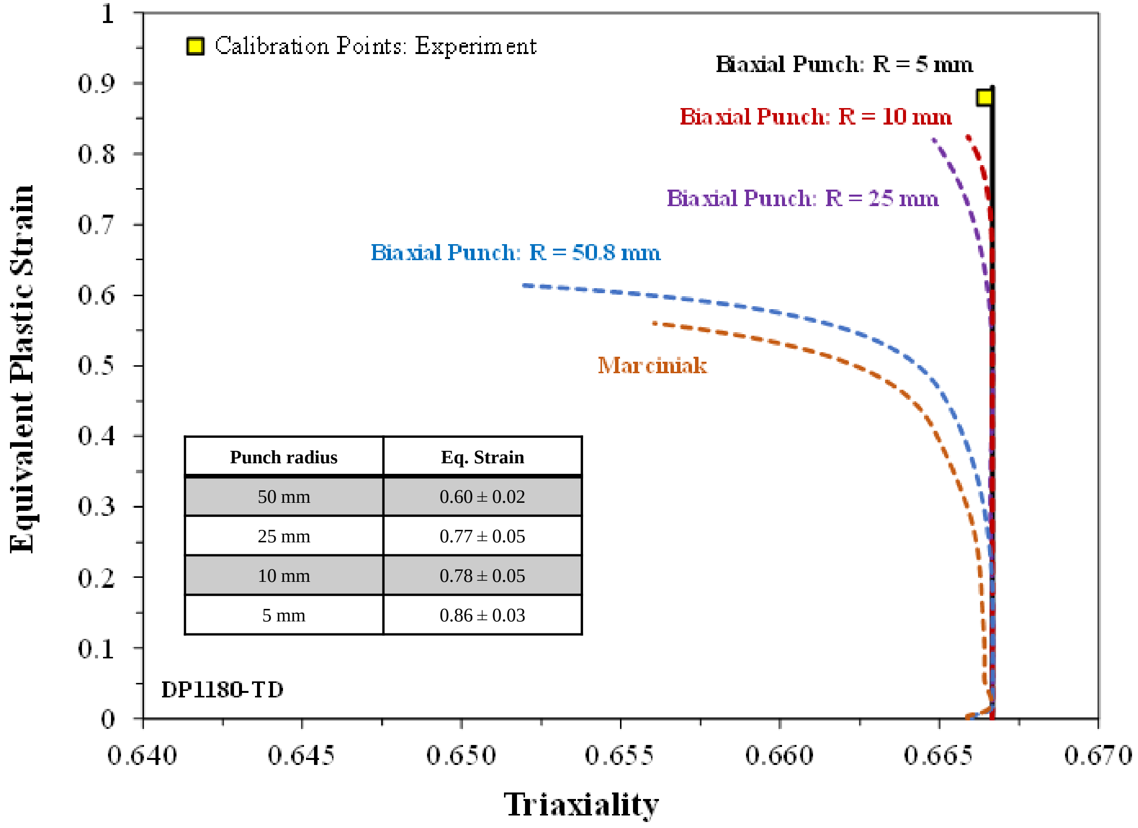

Punch radius	Eq. Strain
50 mm	0.60 ± 0.02
25 mm	0.77 ± 0.05
10 mm	0.78 ± 0.05
5 mm	0.86 ± 0.03

PROPORTIONAL FRACTURE: UNIAXIAL TENSION

Uniaxial tension might be most challenging test due to necking instability and its type of localization

Tensile geometry affects localization mode… the hole tension failed behind edge for DP1180

→ *DIC fracture strains in necking-based samples require thickness correction or are too conservative*

Conical hole expansion (R = 5 mm) with machined hole gave best estimate for DP1180. <u>No necking</u>

Hole expansion methodology and FE verification in Narayanan et al. (2022)

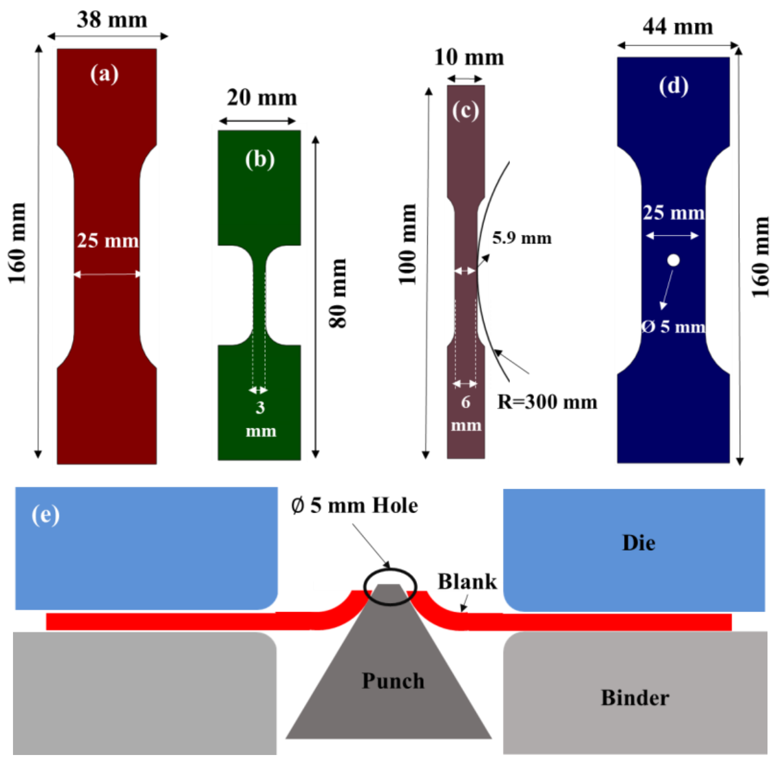

Specimen geometries of (a) JIS No.5. (b) miniature tensile, (c) tapered sub-sized ASTM-E8 tensile (d) central hole tension, and (e) schematic of hole expansion test with machined hole.

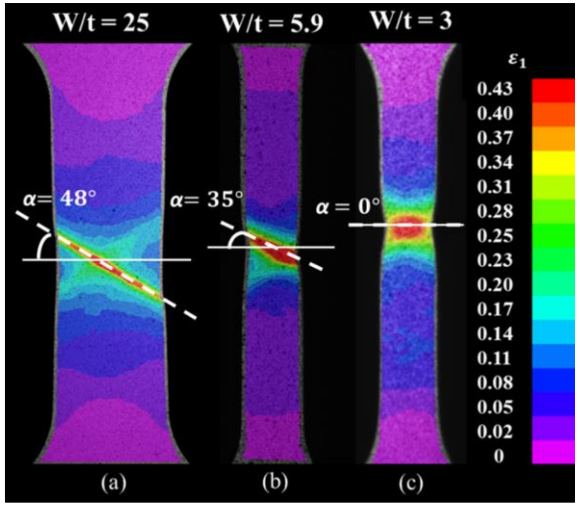

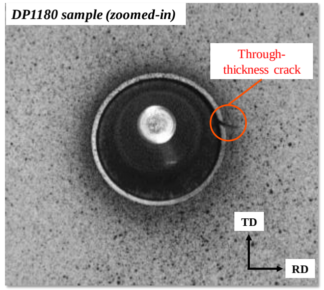

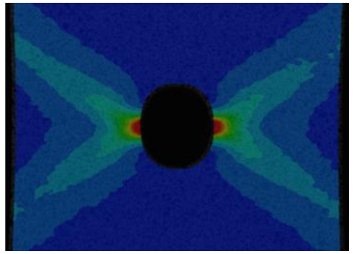

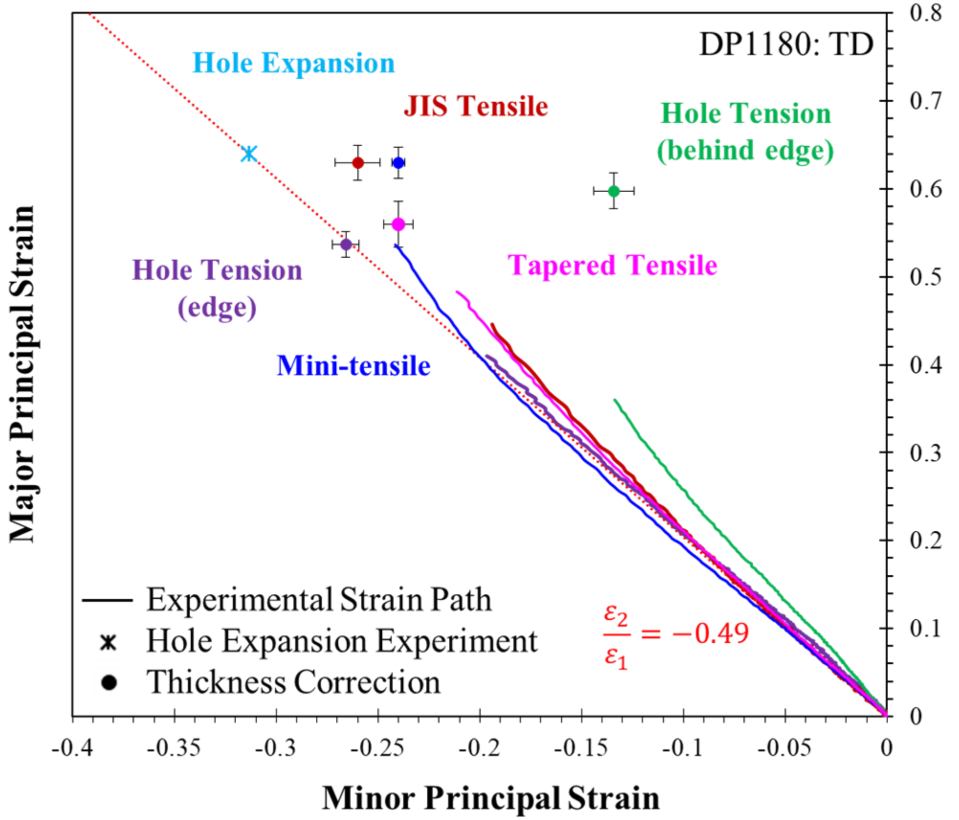

Narayanan, A., Abedini, A., *Khameneh, F., Butcher, C. (2022). *Journal of Materials Engineering and Performance*, https://doi.org/10.1007/s11665-022-07460-6.

CONICAL HOLE EXPANSION FOR UNIAXIAL FRACTURE

Conical hole expansion induces through-thickness strain gradient to suppress necking

Fracture initiates at outer edge that is in uniaxial tension for entire test

Use outer radius to fracture location with image processing. Easy!

Major & Minor Strain

$$\varepsilon_1^\theta = \ln\left(\frac{D_{outer}^\theta}{D_0}\right);\ \varepsilon_2^\theta = -\frac{R_{\theta+90}}{1+R_{\theta+90}}\varepsilon_1^\theta$$

Equivalent Plastic Strain

$$\sigma_{eq}\varepsilon_{eq}^{WC} = \sigma_{\theta+90}\varepsilon_{1,\theta}^{p} \Rightarrow \varepsilon_{eq}^{WC} = \left(\frac{\sigma_{\theta+90}}{\sigma_{eq}}\right)\varepsilon_{1,\theta}^{p}$$

Through-thickness gradients in HET

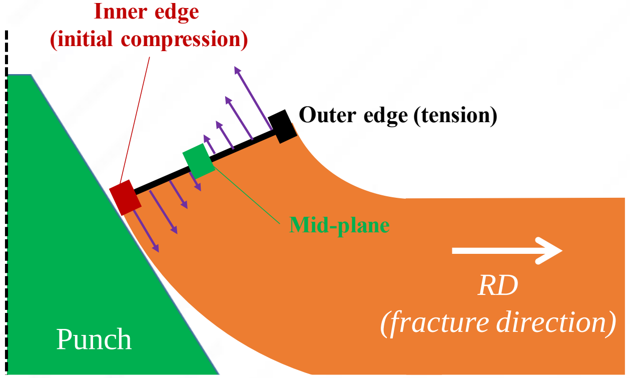

No through-thickness necking

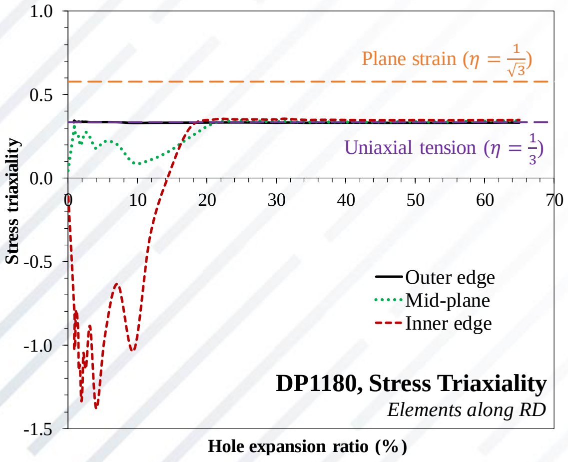

Proportional Strain Path at Outer Edge

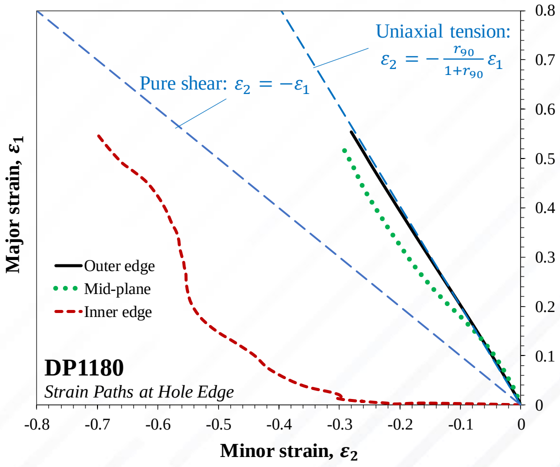

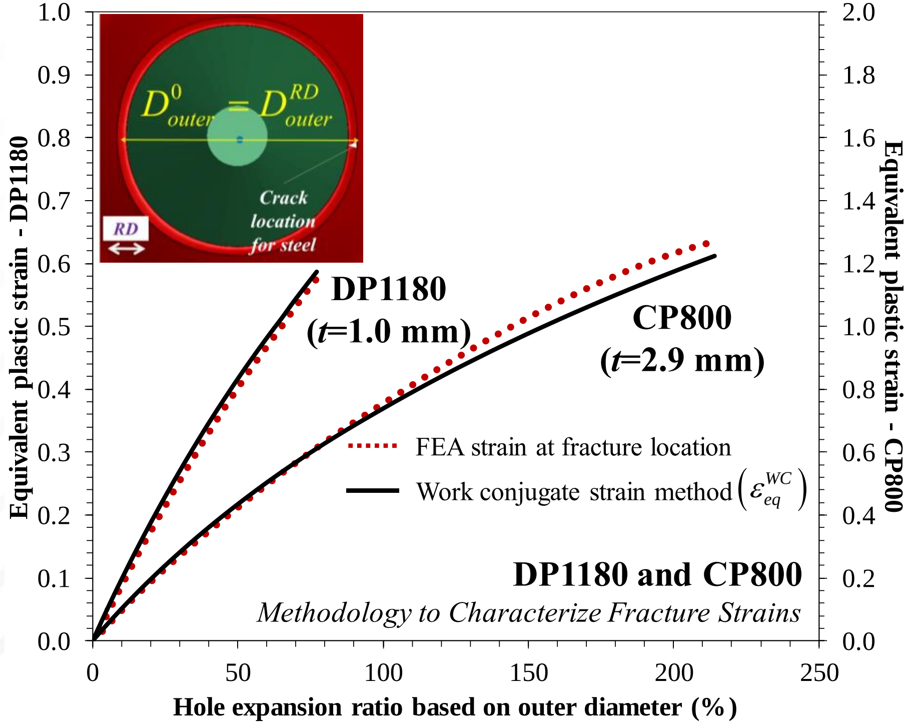

PROPORTIONAL FRACTURE LOCUS

Proportional fracture model calibrated using tests without necking: *Approx. constant triaxiality in plane stress*

All tests analyzed with a consistent virtual strain gauge length (VSGL) of 0.5 mm.

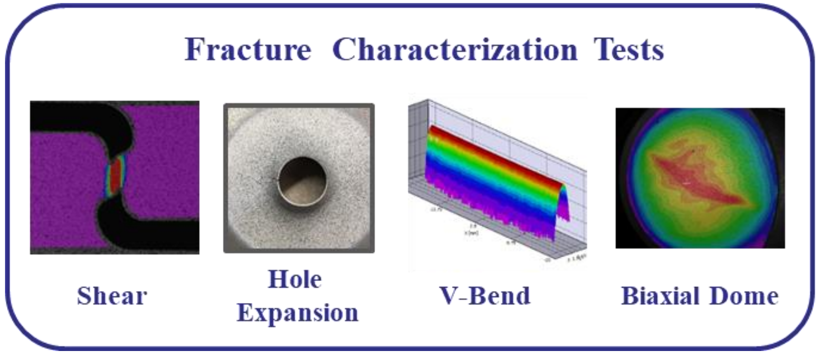

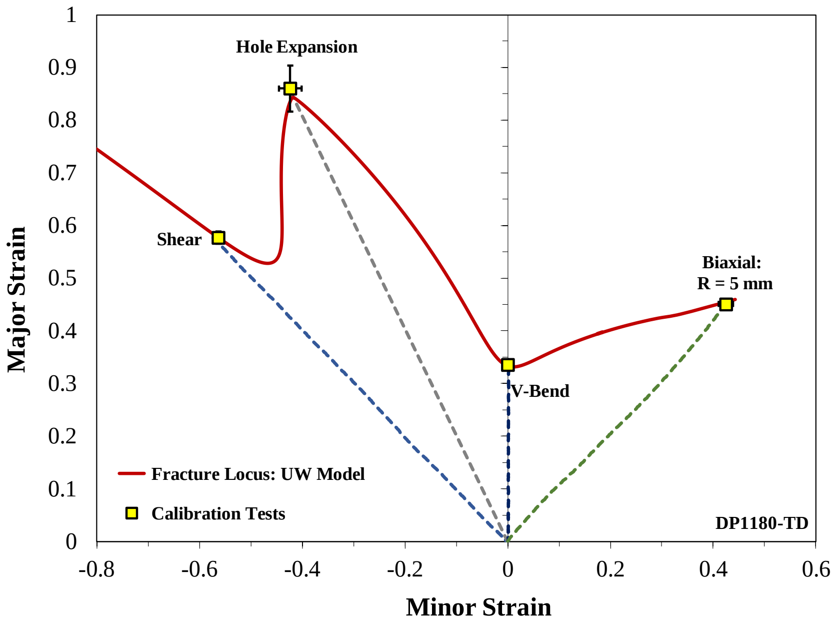

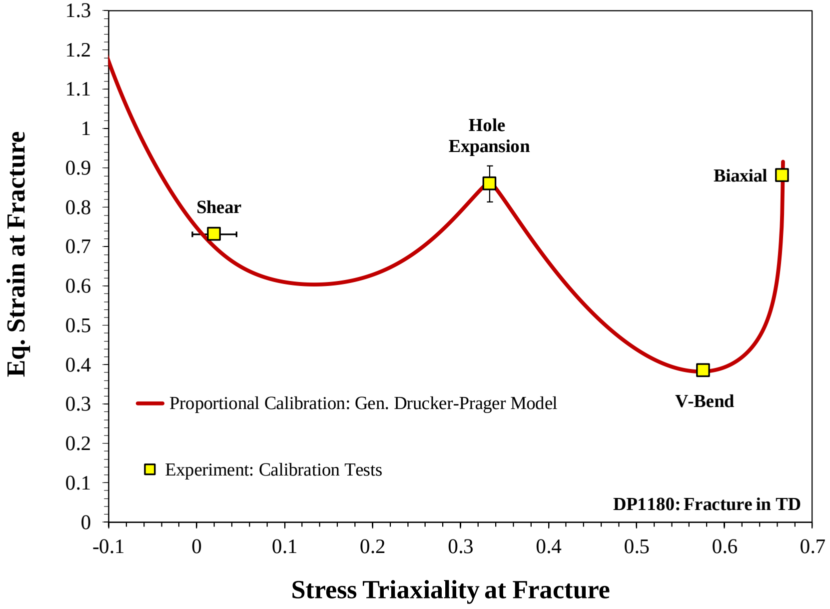

UW Generalized Drucker Prager (GDP) Model:

$$\sigma_1^f\left(m,b,c,d\right)=\frac{b\Phi^{VM}(\bar{\theta}_L,m=2)}{\Phi^{HF}(T,\bar{\theta}_L,m)+c\left(2T+f_1(\bar{\theta}_L)+f_3(\bar{\theta}_L)\right)+f_2(\bar{\theta}_L)d}$$

$$T=\frac{\sigma_{\text{hyd}}}{\sigma_{eq}^{\text{vM}}};\qquad \bar{\theta}=1-\frac{2}{\pi}\cos^{-1}\left(\frac{27}{2}\frac{J_3}{\left(\sigma_{eq}^{\text{vM}}\right)^3}\right)$$

$$\Phi^{HF}(\bar{\theta}_L,m)=\frac{\sigma_{\text{eq}}}{\sigma_1}=\left(\frac{1}{2}\left(f_1-f_2\right)^m+\frac{1}{2}\left(f_2-f_3\right)^m+\frac{1}{2}\left(f_3-f_1\right)^m\right)^{\frac{1}{m}}$$

FRACTURE IN BI-LINEAR STRAIN PATHS

How do the fracture strains vary in non-proportional loading?

In-Plane Pre-straining in uniaxial, plane strain and biaxial conditions

Select secondary fracture tests <u>without necking</u> and approx. linear strain paths

Major experimental effort: > 250 tests performed. Subset of data provided for NUMISHEET 2022 Benchmark

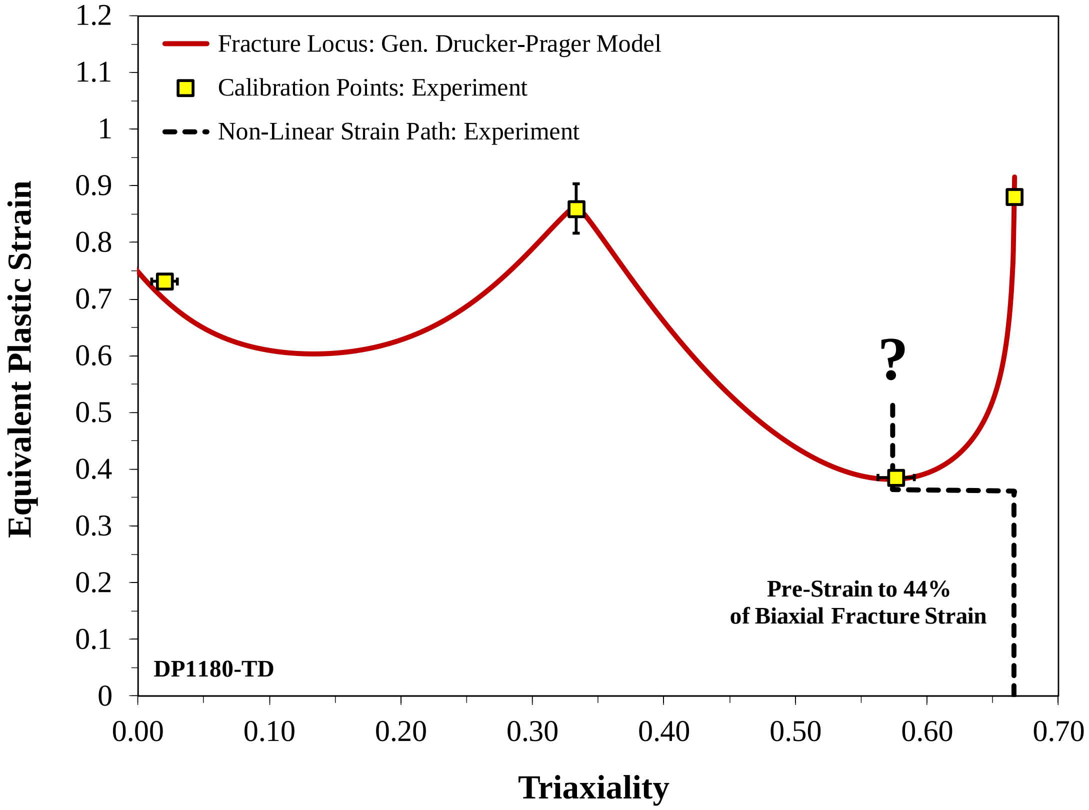

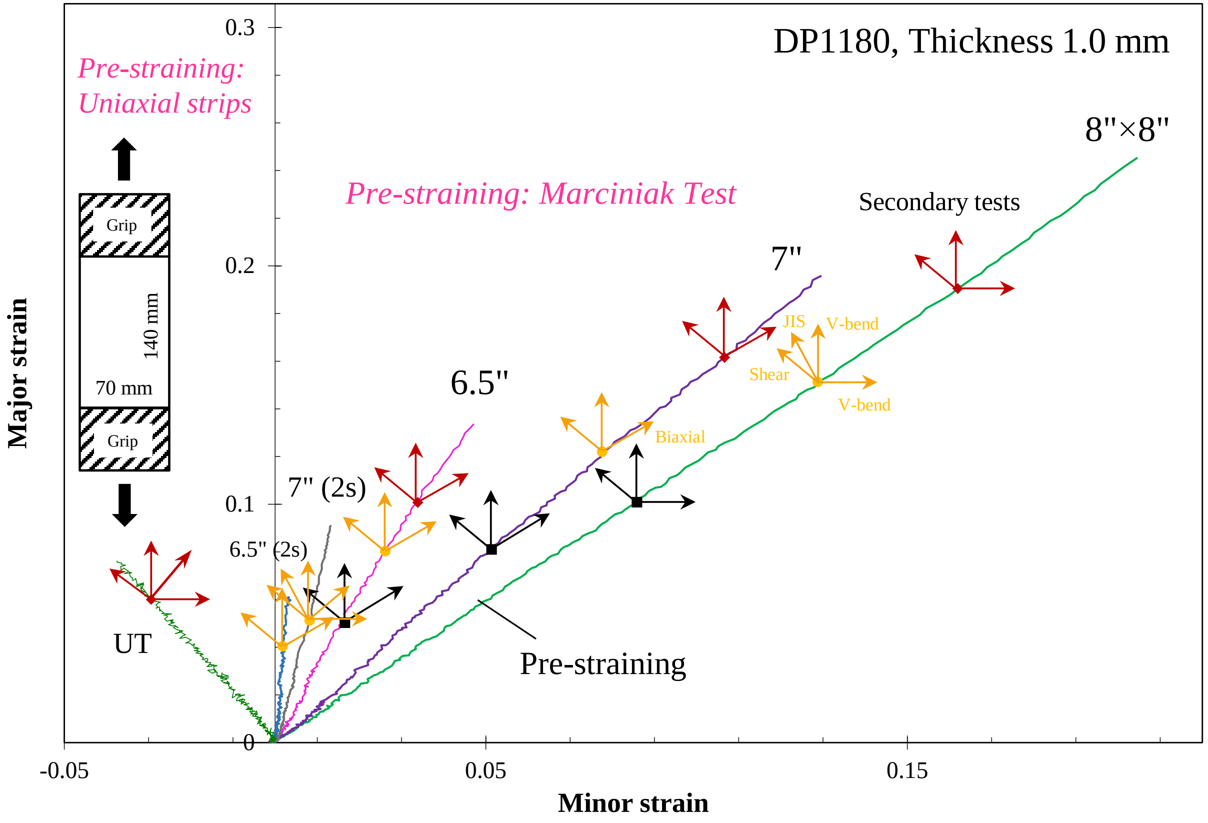

FIRST STAGE: IN-PLANE PRE-STRAINING

Uniaxial Pre-Straining: Oversized rectangular samples (strain variation < 1%)

Plane Strain & Biaxial Pre-Straining: Marciniak tests   (strain variation of 2% or less)

Local DIC strain history tracked for mapping to secondary fracture tests

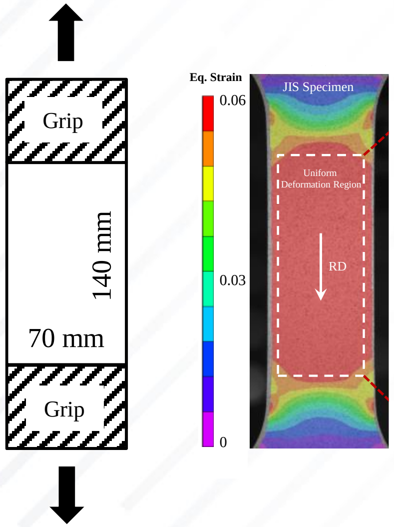

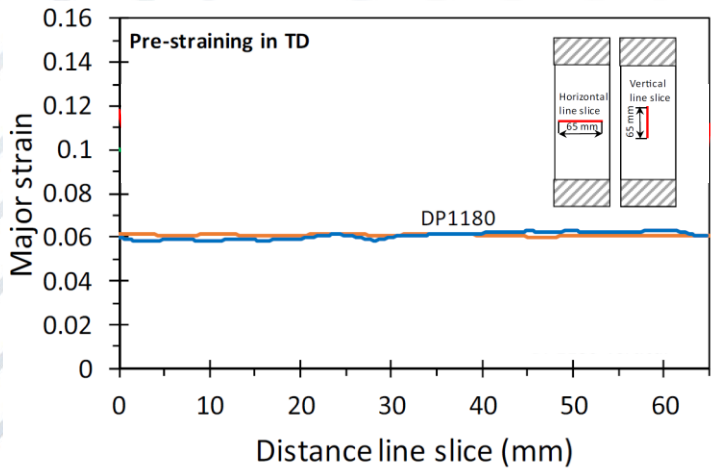

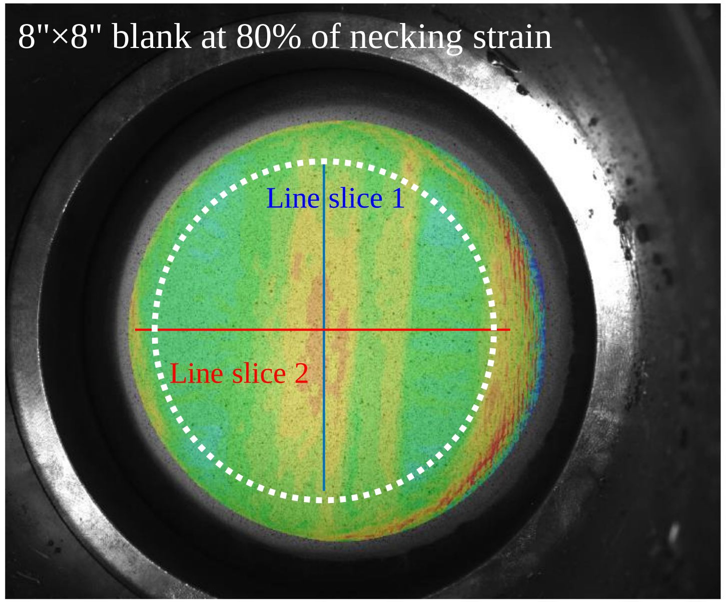

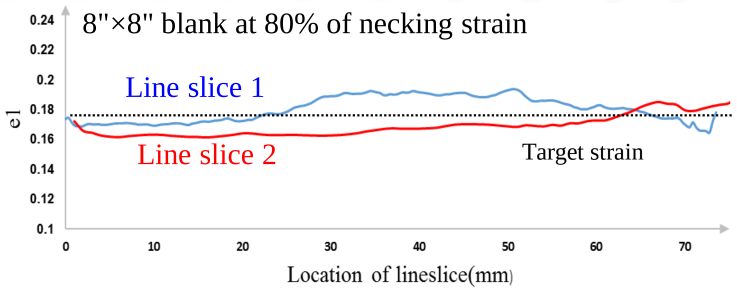

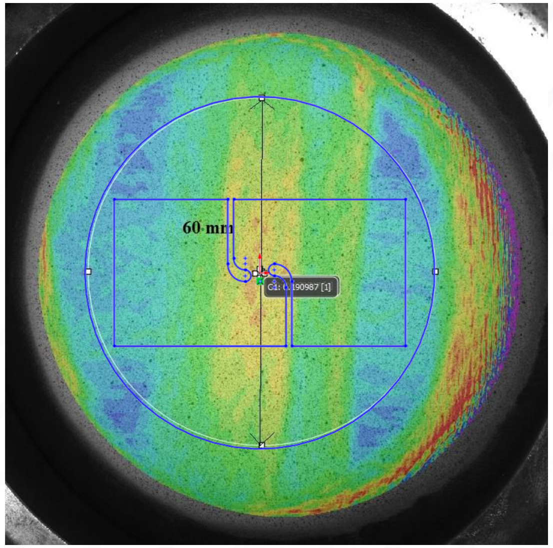

Demonstration of shear gage region centered on Marciniak test of DP1180

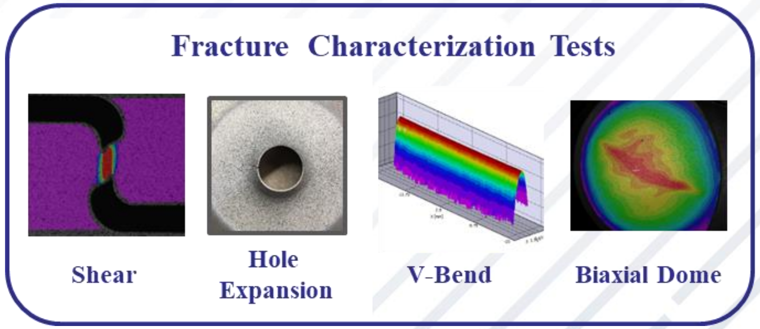

SELECT NLSP DATA: V-BEND AFTER PLANE STRAIN STRETCH

Fracture strains constant for plane strain stretch + plane strain bend

Convergence – highlights plane strain fracture was accurately characterized

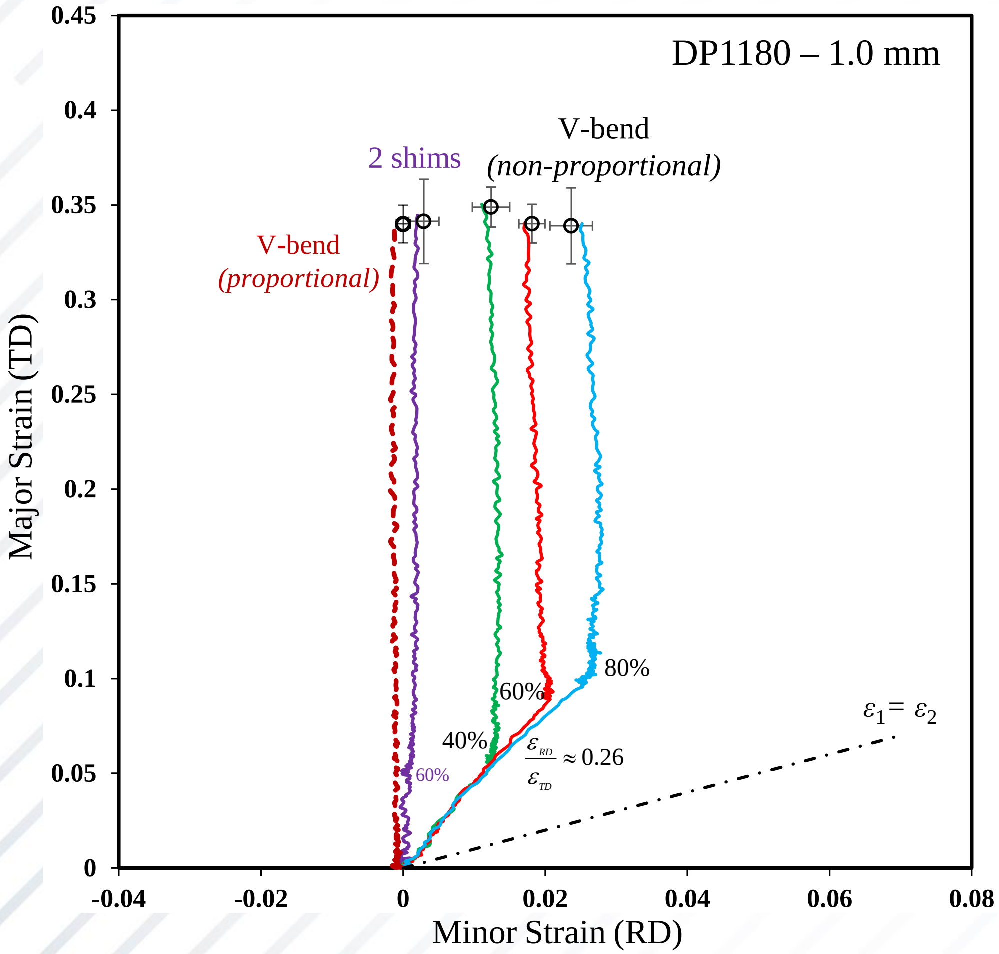

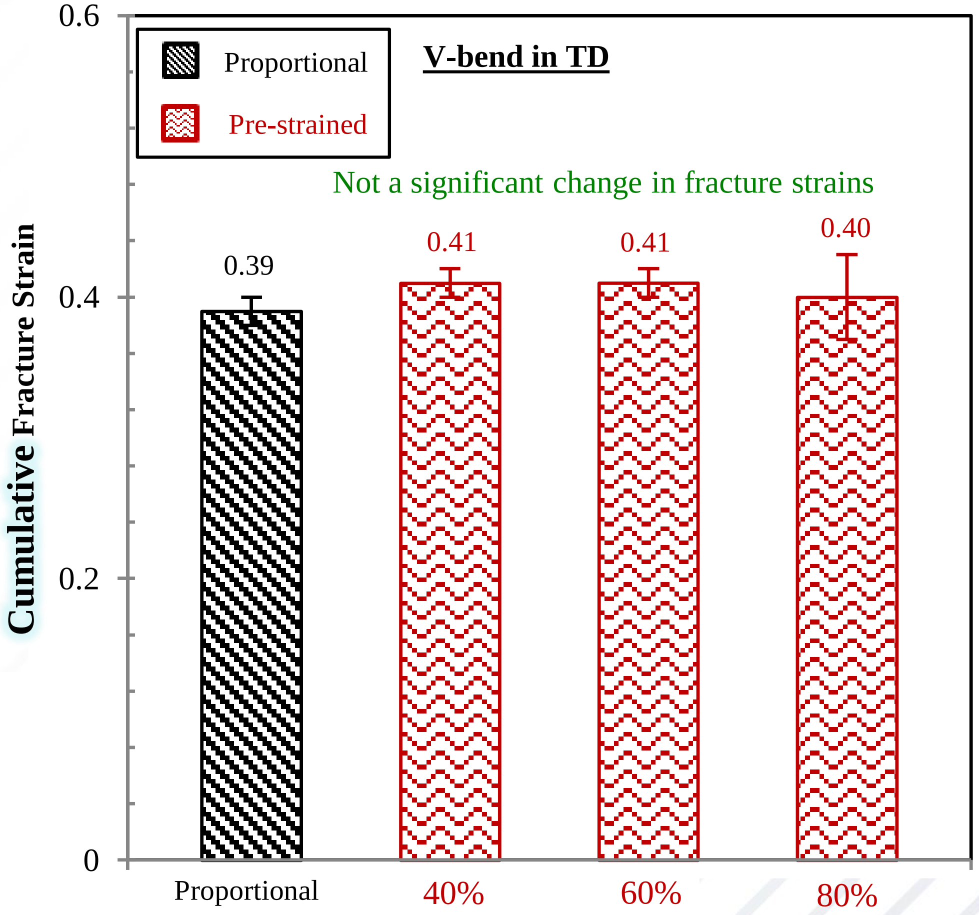

SELECT NLSP DATA: V-BEND AFTER BIAXIAL STRETCH

Repeatable strain paths and fracture strains

Comparable major principal strain at fracture in different strain paths

Cumulative equivalent fracture strain increases with biaxial pre-straining

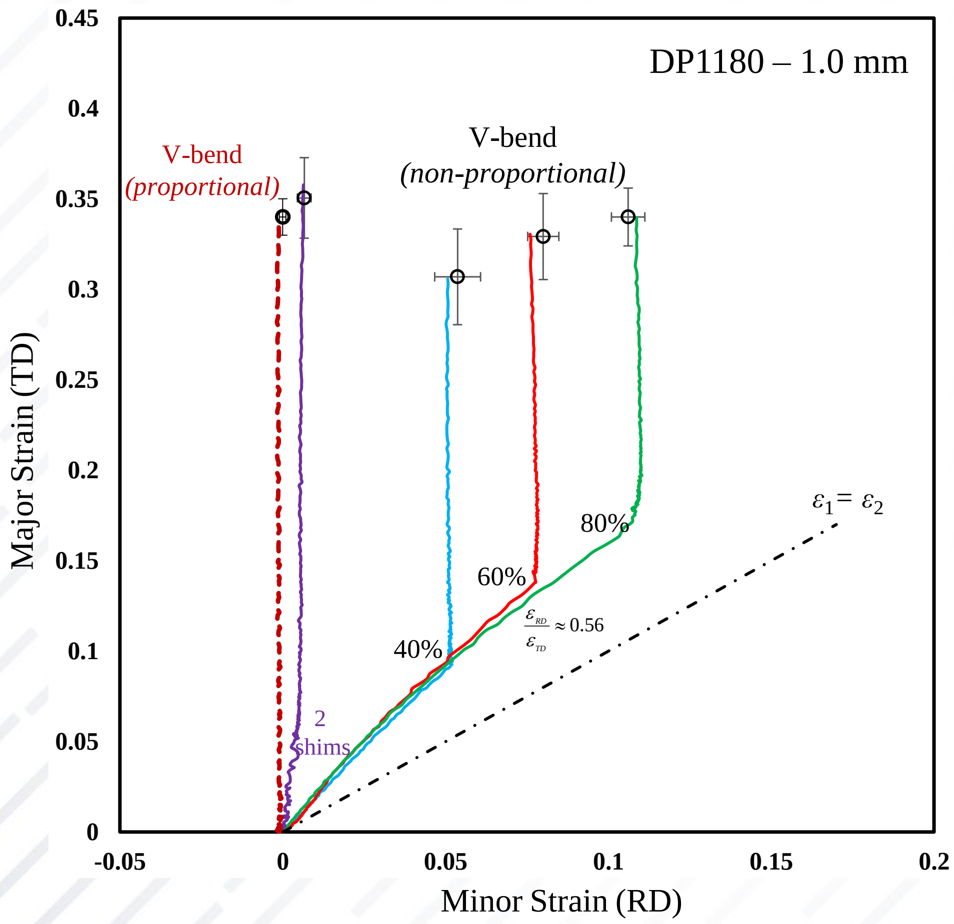

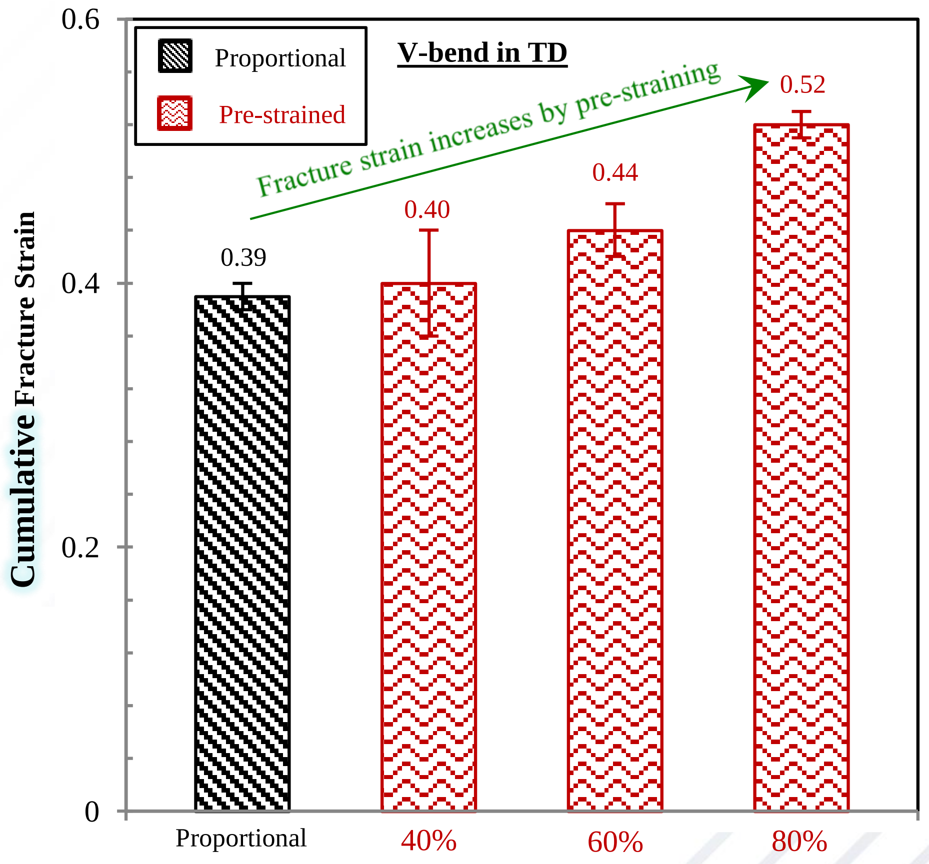

SELECT NLSP DATA: SHEAR AFTER BIAXIAL STRETCH

GDIS

Repeatable strain paths and fracture strains

Cumulative equivalent fracture strains in shear increase with biaxial stretch

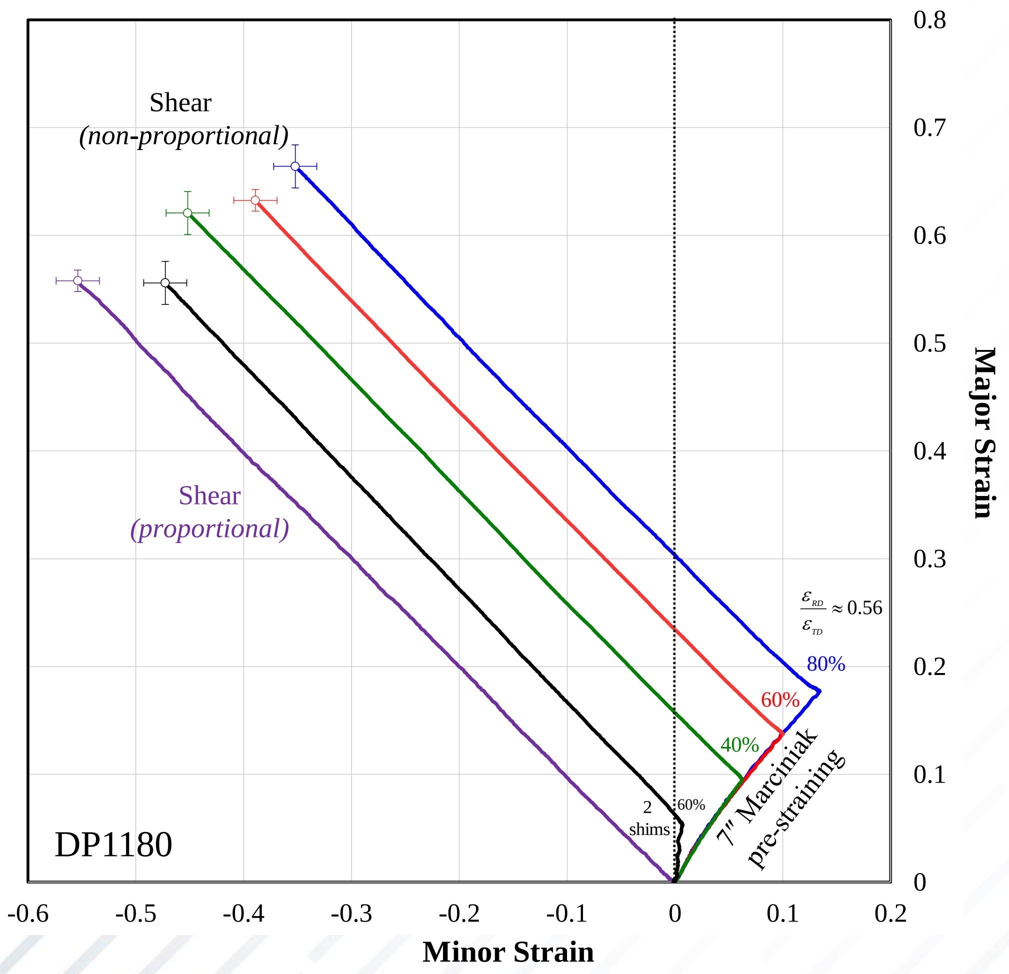

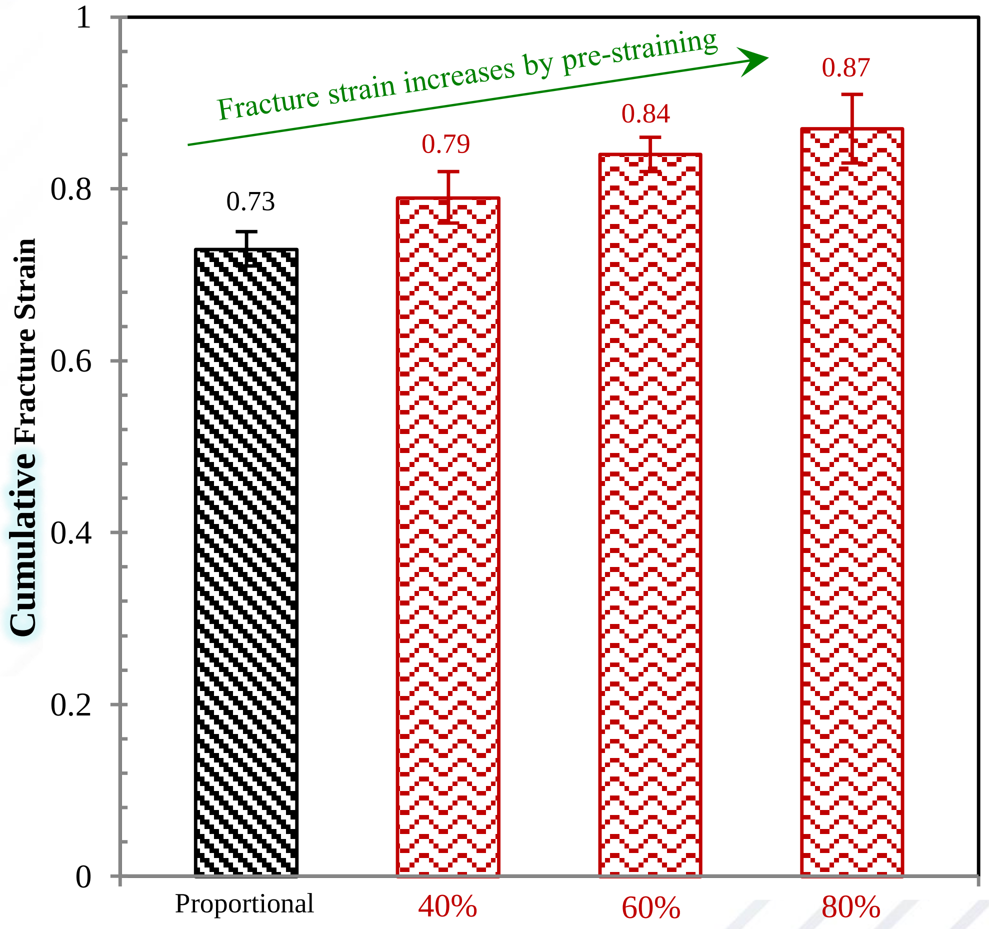

DAMAGE ACCUMULATION AND FRACTURE MODELS:

APPLYING PROPORTIONAL FRACTURE DATA TO NON-LINEAR STRAIN PATHS

All models are equally valid in proportional loading… but what happens in non-proportional loading?

Stress-based representations do not require a damage counter: $\sigma_1 > \sigma_1^f(T,L)$

Equivalent strain representations employ phenomenological damage models (no physical foundation)

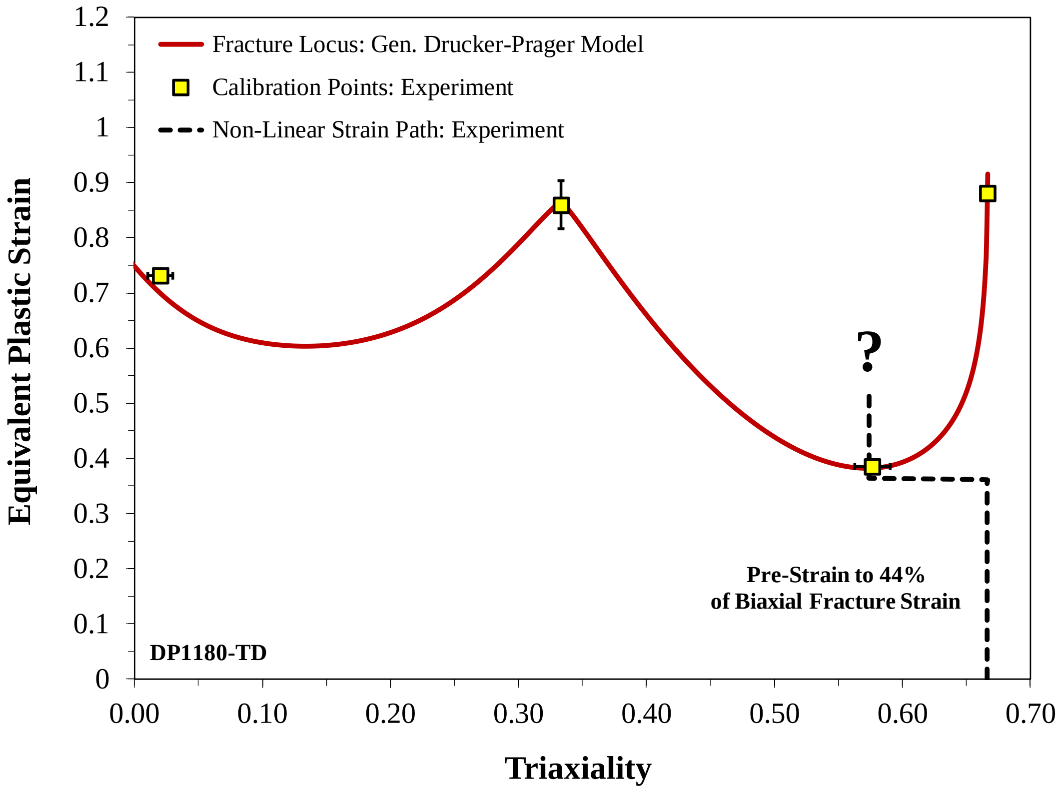

Linear damage (Johnson & Cook, 1983) commonly used

$$D = \int \frac{d\varepsilon_{eq}}{\varepsilon_f(T,L)} \qquad Fracture: \ D = 1$$

Power Law Damage (Xue, 2007)

$$\frac{\Delta D}{\Delta \varepsilon_{eq}^p} = \frac{n_D}{\varepsilon_f(T,L)} \boxed{\left(\frac{\varepsilon_{eq}^p}{\varepsilon_f(T,L)}\right)^{n_D(1-1/n_D)}} \qquad D^{prop.} = \left(\frac{\varepsilon_{eq}^p}{\varepsilon_f(T,L)}\right)^{n_D}$$

GISSMO: Based on Power Law but implemented differently

$$\frac{\Delta D^{GISSMO}}{\Delta \varepsilon_{eq}^p} = \frac{n_D}{\varepsilon_f(T,L)} \boxed{D}^{(1-1/n_D)}$$

$D_{initial} \neq 0$,

LS-DYNA uses $D_{initial} = 1.0e^{-20}$

Neukamm, F., Feucht, M., Haufe, A. Consistent damage modelling in the process chain of forming to crashworthiness simulations. LS-DYNA Anwenderforum, Bamberg 2008

Xue, L., (2007). International Journal of Solids and Structures 44,

DAMAGE ACCUMULATION EXAMPLE: DP1180

In-Plane Biaxial Pre-strain to Plane Strain Bending (change from highest to lowest fracture strains)

GISSMO overestimated fracture. Linear slightly better than non-linear with recommended n = 2

Power Law damage was conservative. Influence of exponent can be different than GISSMO

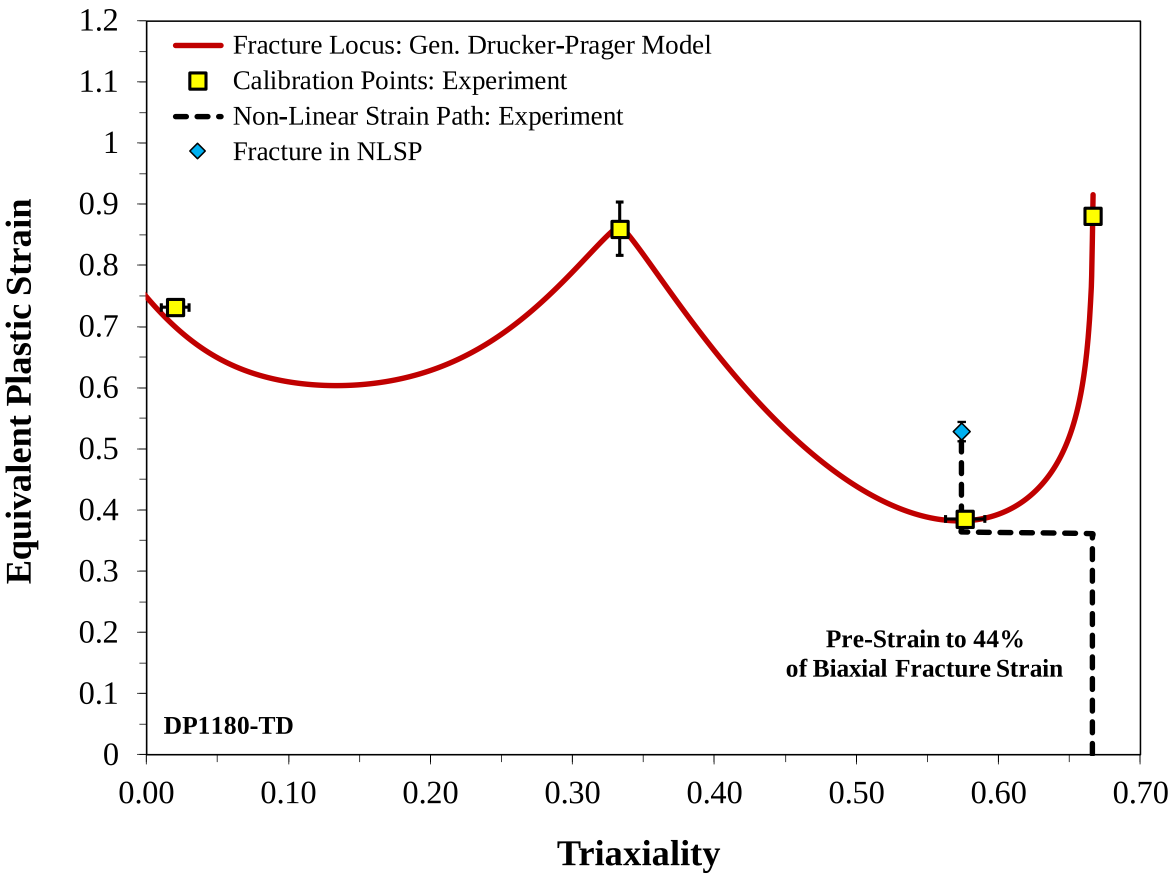

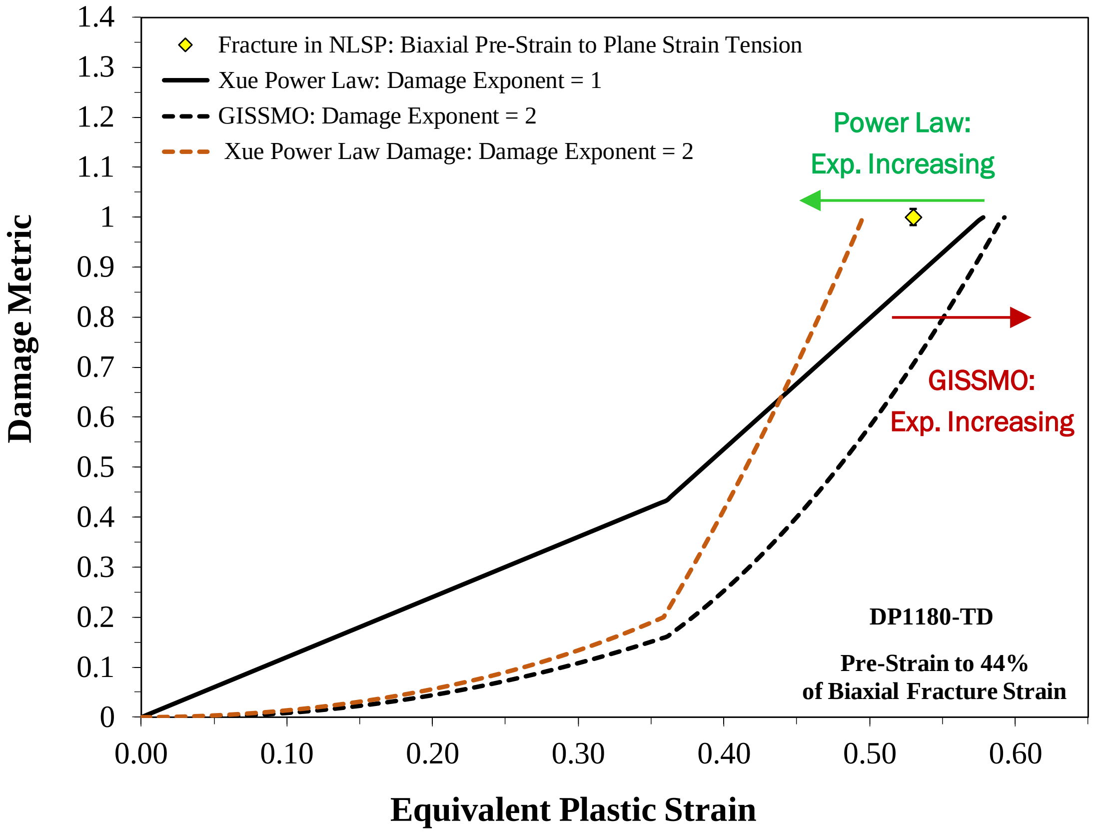

DAMAGE ACCUMULATION EXAMPLE 2: DP1180

GDIS

Plane Strain Pre-Strain followed by Biaxial punch (path change from lowest to highest fracture strains)

GISSMO underestimated fracture. Non-linear did better by reducing influence of first path in plane strain

Power Law Damage similar to GISSMO when going from severe-to-mild stress state

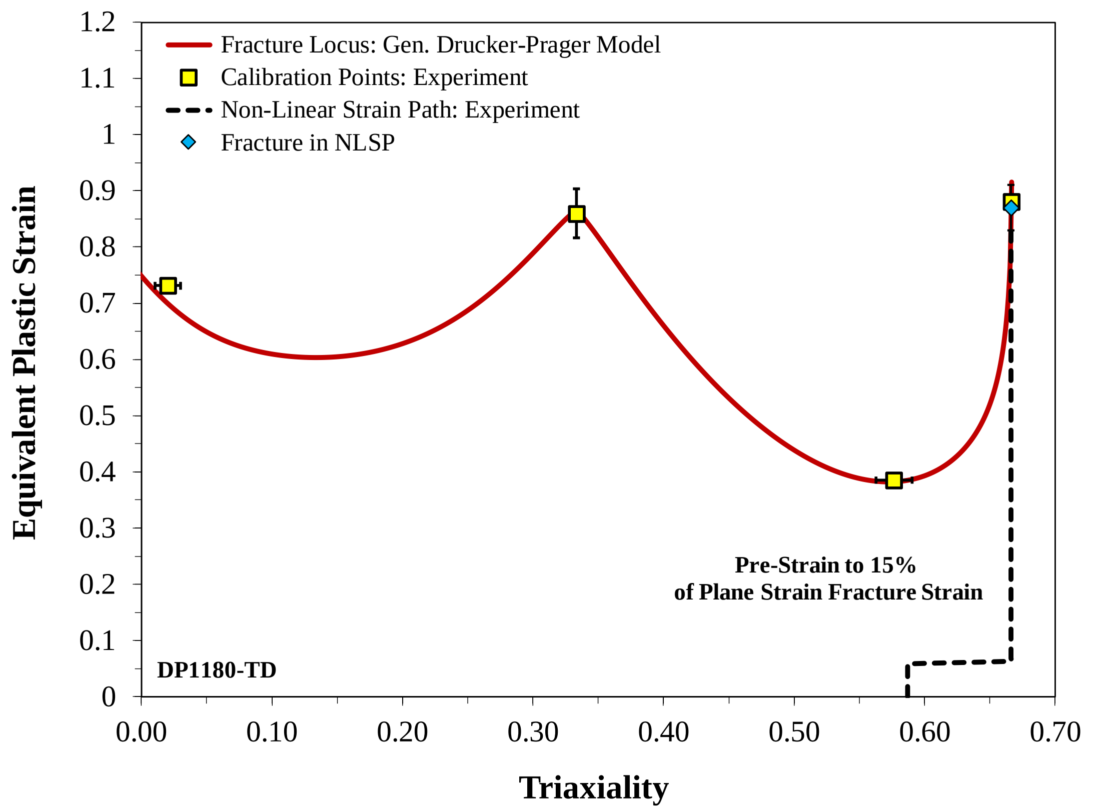

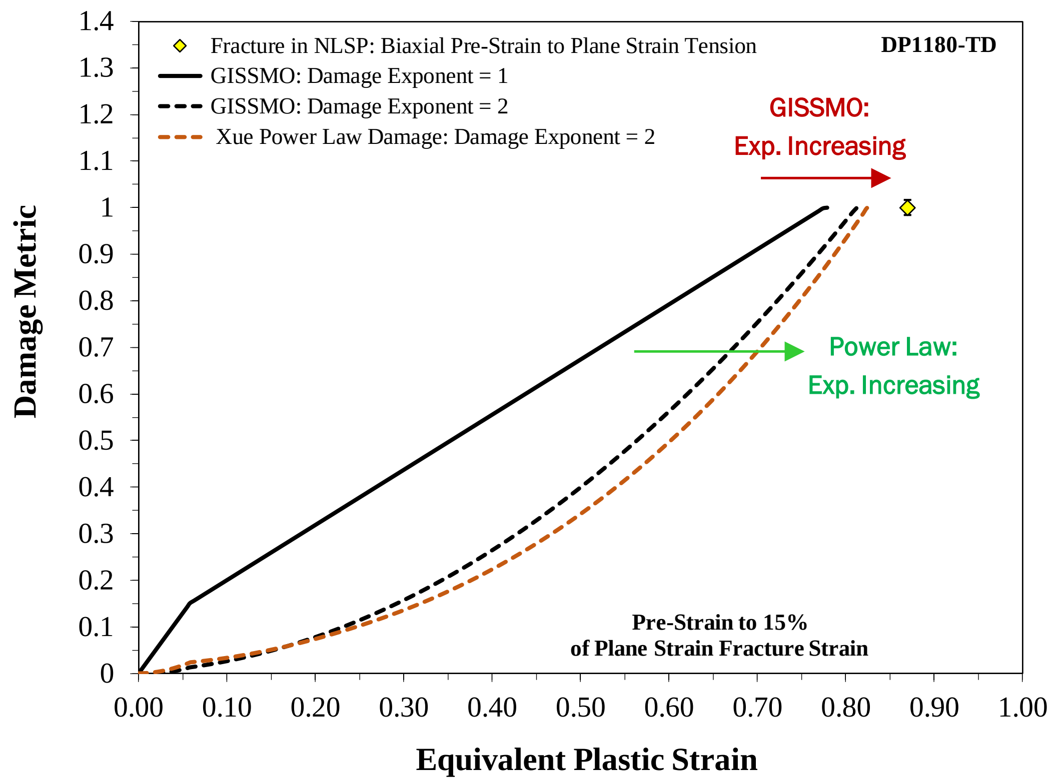

EVALUATION OF FRACTURE LOCUS: GISSMO

Evaluate all non-linear strain path tests: 3 Fracture Loci with 4 parameters calibrated from 4 data points

Paired with GISSMO damage model using n = 2

Define correlation metric to evaluate model predictions

$$D = \frac{\varepsilon^{f}_{eq-\text{Predicted}}}{\varepsilon^{f}_{eq-\text{Test}}} \qquad D = 1 \quad \text{Perfect correlation}$$

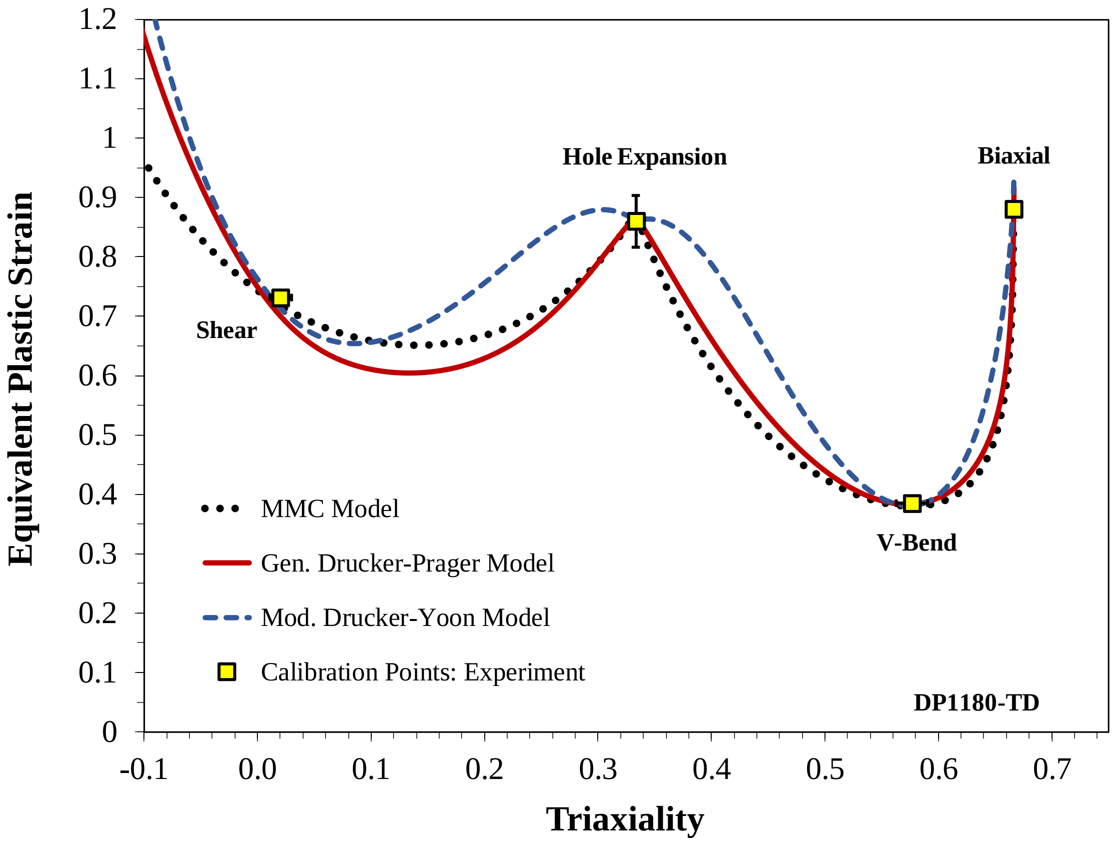

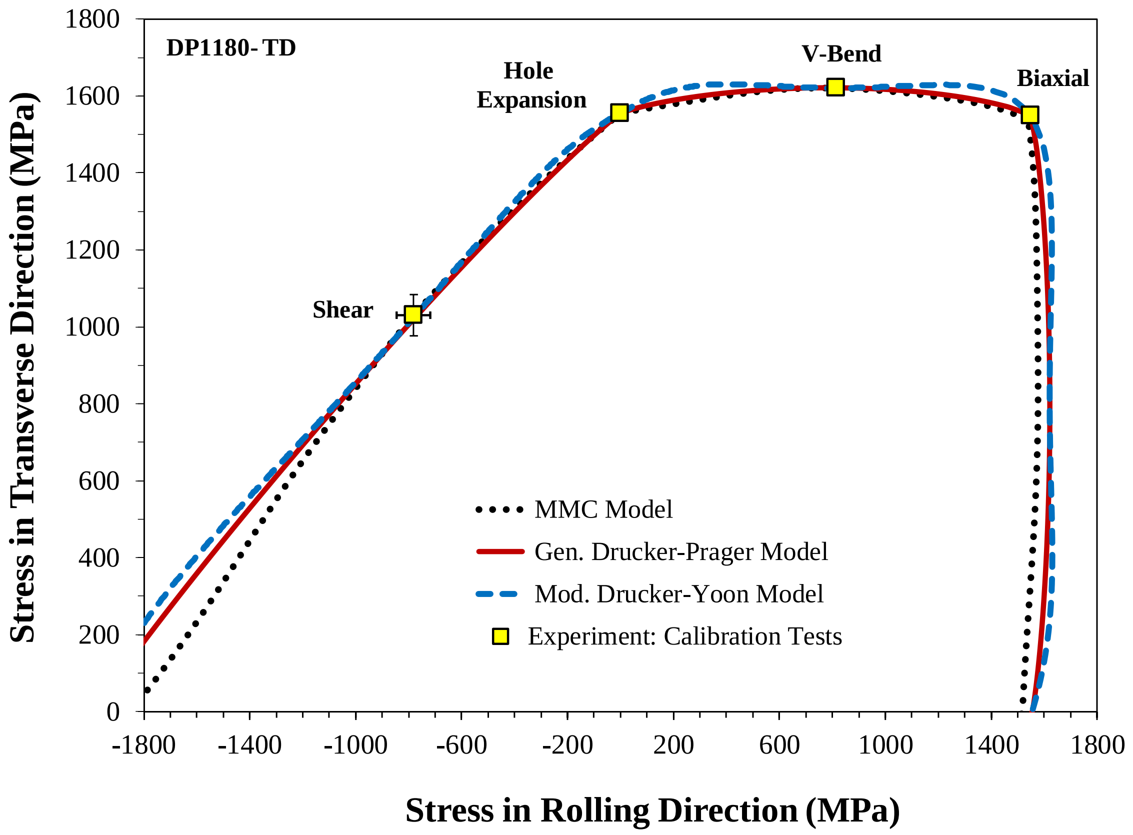

EVALUATION OF FRACTURE LOCUS: GISSMO*

Select Generalized Drucker-Prager model (marginally better)

MMC model rather conservative for second stage biaxial loading

Drucker-Yoon model overestimated fracture in second stage shear

$$D = \frac{\varepsilon^{f}_{eq-\text{Predicted}}}{\varepsilon^{f}_{eq-\text{Test}}} \qquad D = 1 \quad \text{Perfect correlation}$$

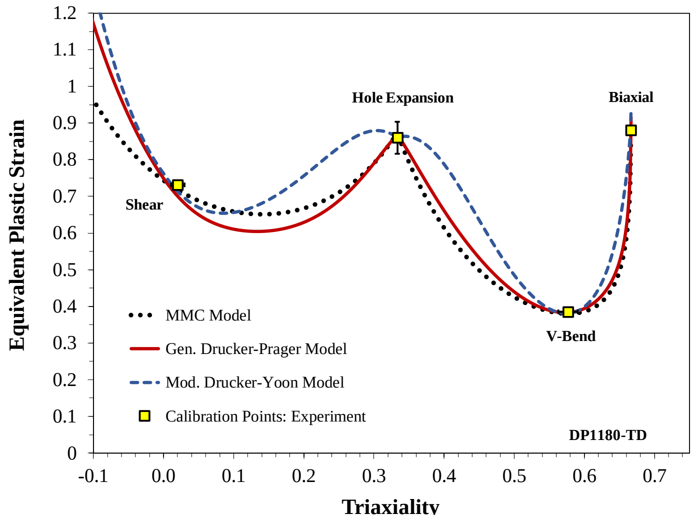

Damage Model		GISSMO Damage Model: *Damage Exponent = 2*					
Damage Metric & Parameters		Modified Mohr-Coulomb Model		Gen. Drucker-Prager Model		Mod. Drucker-Yoon Model	
Fracture Metric:	$\varepsilon_f^{\text{model}} / \varepsilon_f^{\text{exp}}$	Average	Std. Dev	Average	Std. Dev	Average	Std. Dev
Secondary Path	Plane Strain Tension (12 Paths)	1.08	± 0.08	1.09	± 0.08	1.11	± 0.09
	Biaxial Stretching (9 Paths)	0.89	± 0.02	0.95	± 0.02	1.02	± 0.02
	Shear (12 Paths)	0.98	± 0.09	0.97	± 0.08	1.13	± 0.12
	Uniaxial Tension (12 Paths)	0.93	± 0.07	0.93	± 0.06	0.94	± 0.06

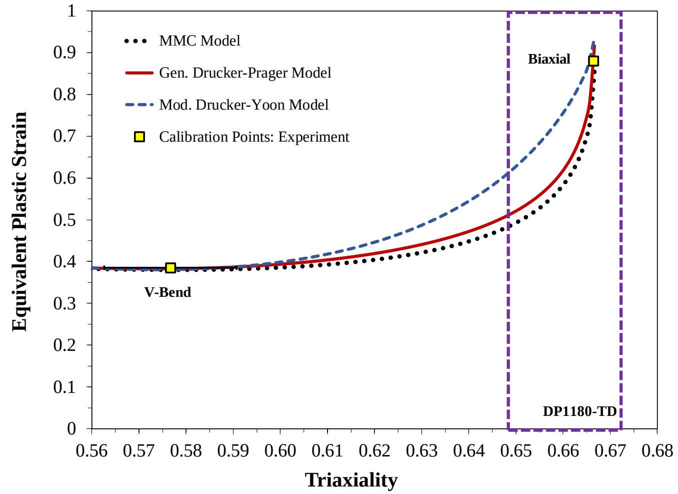

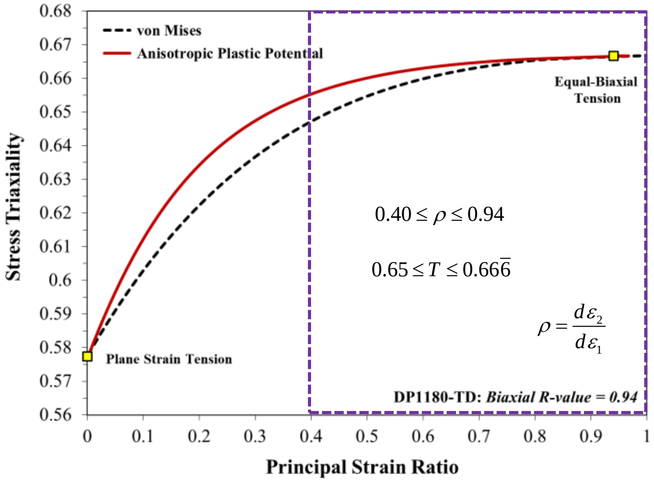

Asymptotic behavior in biaxial tension

→ Triaxiality has poor resolution

→ Consider additional biaxial tests and use NLSP due to necking as evaluation

*Results also depend upon choice of damage model and calibration of loci

FRACTURE REPRESENTATIONS: DP1180

→ *All NLSP fracture data showed with terminal values*

→ Principal Stress representation has apparent convergence

→ Eq. strain representation shows sensitivity to hardening model

→ Proportional fracture locus of DP1180 appears conservative in NLSP.

→ Need to evaluate damage models

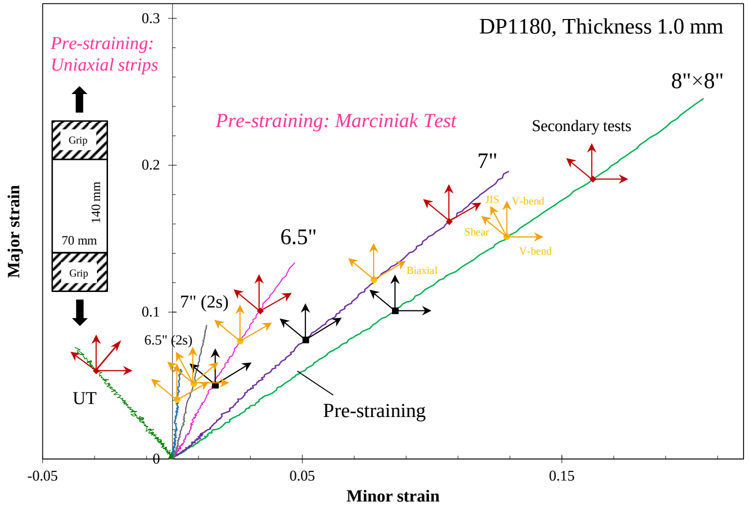

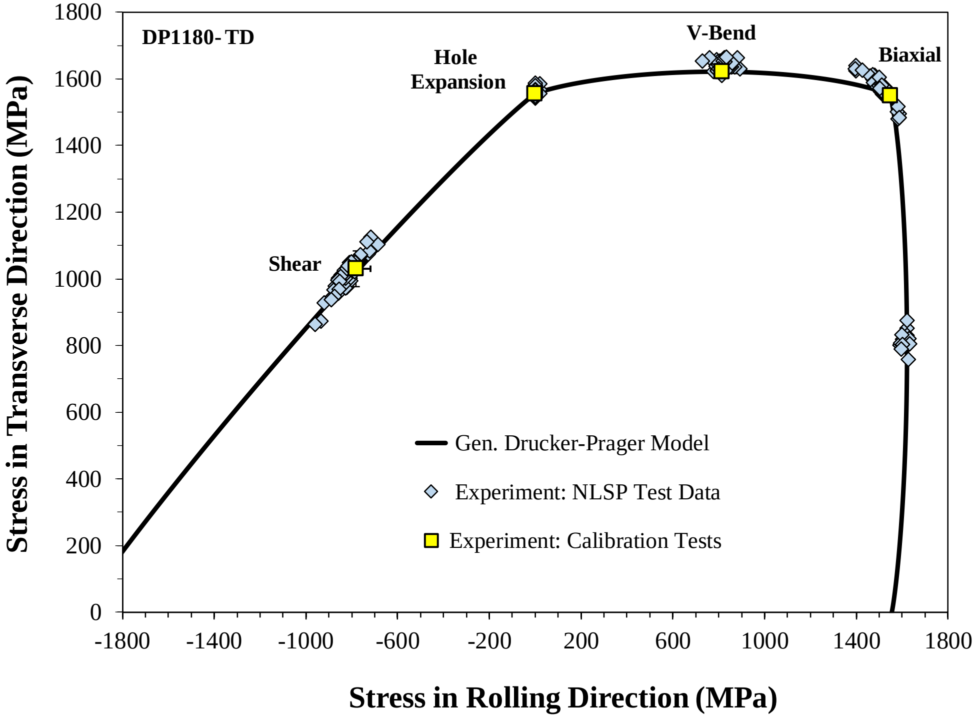

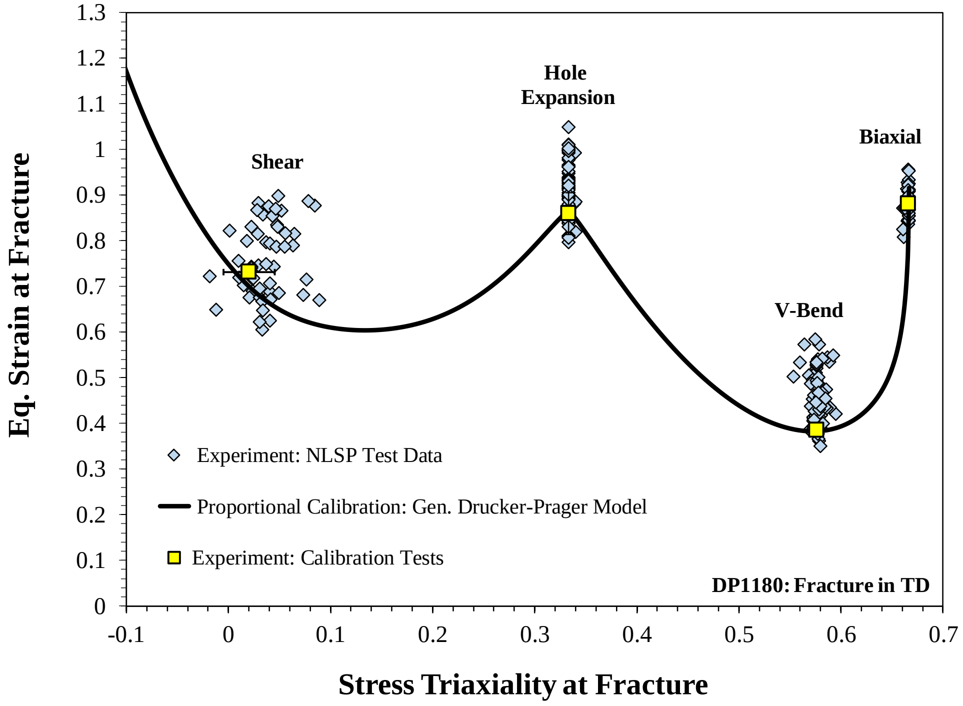

GISSMO DAMAGE MODEL EVALUATION

GDIS

GISSMO Damage Accumulation:

$$D = \int \frac{n_D}{\varepsilon_f(T)} D^{(1-1/n_D)} d\varepsilon_{eq}^{p}$$

Assume Damage exponent : $n_D = 1, 2$

Advantages: Widely used and available in LS-DYNA, Linear form = Johnson-Cook model
Eq. Strain based (relatively convenient)

Disadvantages: No physical foundation – user assumes damage exponent;
Damage accumulation unrelated to hardening ability

Damage Model		GISSMO			
Damage Metric & Parameters		Eq. Strain *Damage Exponent = 1*		Eq. Strain *Damage Exponent = 2*	
Fracture Metric: $\varepsilon_f^{\text{model}} / \varepsilon_f^{\text{exp}}$		Average	Std. Dev	Average	Std. Dev
Secondary Path	Plane Strain Tension (12 Paths)	1.05	± 0.08	1.09	± 0.08
	Biaxial Stretching (9 Paths)	0.91	± 0.02	0.95	± 0.02
	Shear (12 Paths)	0.94	± 0.08	0.97	± 0.08
	Uniaxial Tension (12 Paths)	0.90	± 0.06	0.93	± 0.06

Observations: Recommended non-linear damage (n = 2) performed better than linear damage (Johnson-Cook)
→ Linear damage more conservative and will predict more fracture in FEA
→ *Non-linear GISSMO over-predicted when switching to path with lower fracture strain (localization...)*

POWER LAW DAMAGE MODEL EVALUATION

GDIS

Power Law Damage Accumulation:

$$D = \int \frac{n_D}{\varepsilon_f(T)} \left(\frac{\varepsilon_{eq}^p}{\varepsilon_f(T)} \right)^{n_D - 1} d\varepsilon_{eq}^p$$

Assume Damage exponent : $n_D = 1, 1.5, 2$

Advantages: Appears to be consistent version of damage model GISSMO was based upon

Equivalent to GISSMO and Johnson-Cook for Linear Damage

Disadvantages: Same as GISSMO - No physical foundation – user assumes damage exponent

Damage accumulation unrelated to hardening ability

Damage Model		GISSMO				Power Law Damage					
Damage Metric & Parameters		Eq. Strain *Damage Exponent = 1*		Eq. Strain *Damage Exponent = 2*		Eq. Strain *Damage Exponent = 1*		Eq. Strain *Damage Exponent = 1.5*		Eq. Strain *Damage Exponent = 2*	
Fracture Metric: $\varepsilon_f^{\text{model}} / \varepsilon_f^{\text{exp}}$		Average	Std. Dev	Average	Std. Dev	Average	Std. Dev	Average	Std. Dev	Average	Std. Dev
Secondary Path	Plane Strain Tension (12 Paths)	1.05	± 0.08	1.09	± 0.08	1.05	± 0.08	0.99	± 0.05	0.96	± 0.05
	Biaxial Stretching (9 Paths)	0.91	± 0.02	0.95	± 0.02	0.91	± 0.02	0.95	± 0.02	0.96	± 0.03
	Shear (12 Paths)	0.94	± 0.08	0.97	± 0.08	0.94	± 0.08	0.94	± 0.09	0.94	± 0.09
	Uniaxial Tension (12 Paths)	0.90	± 0.06	0.93	± 0.06	0.90	± 0.06	0.93	± 0.06	0.94	± 0.06

Observations: Performed superior to GISSMO with n = 1.5 – 2.0 recommended for DP1180

→ Significant improvement in predicting failure when second path is more severe as in localization

→ Overall, slightly conservative across all NLSP while GISSMO was not

CONCLUSIONS AND FUTURE WORK

Fracture Characterization

→ Accurate plasticity model is required to differentiate stress states

→ **Select proportional characterization tests without necking for fracture calibration**

→ Choice of fracture loci and calibration is important: ***Biaxial region is critical.***

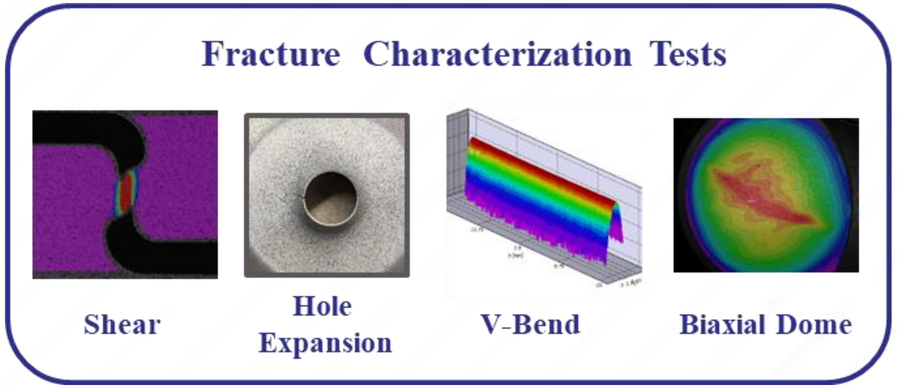

Fracture Models: (Targeted for GDIS2024)

→ Linear damage relatively conservative for fracture of DP1180

→ Power law damage model superior to GISSMO for non-linear damage

→ Investigate anisotropic fracture and application to higher ductility steel

→ Consider physically-based alternate models: Stress and/or plastic work based

ADDITIONAL INFORMATION: PUBLICATIONS FOR DP1180

[1] Abedini, A., Noder, J., Kohar, C.P., Butcher, C. (2020). Accounting for Shear Anisotropy and Material Frame Rotation on Constitutive Characterization of Automotive Alloys. *Mechanics of Materials*, 148, 1-17.

[2] Butcher, C., Jeyranpourkhameneh, J., Abedini, A., Connolly, D., Kurukuri, S. (2021). On the Experimental Characterization of Sheet Metal Formability and the Consistent Calibration of the MK Model for Biaxial Stretching in Plane Stress. *Journal of Materials Processing Technology*, 287, 1-18.

[3] Khameneh, F., Abedini, A, Butcher, C. (2021). Lengthscale effects in optical strain measurement for fracture characterization in simple shear. *International Journal of Fracture* 232, 153-180

[4] Naryanan, A., Abedini, A., Khameneh, F., Butcher, C. (2022). An Experimental Methodology to Characterize the Uniaxial Fracture Strain of Sheet Metals using the Conical Hole Expansion Test. *Journal of Materials Engineering and Performance*, JMEP-21-10-25894. Accepted June 2022. In-Press. Pp. 28.

[5] Fast-Irvine, J.C., Abedini, A., Noder, J., Butcher, C. (2021). An Experimental Methodology to Characterize the Plasticity of Sheet Metals from Uniaxial to Plane Strain Tension. *Experimental Mechanics*, 61, 1381-1404.

[6] Noder, J., Gutierrez, J., Zhumagulov, A., Khameneh, F., Butcher, C. (2021). A Comparative Evaluation of Third Generation AHSS for Automotive Forming and Crash Applications. *Materials*, 14, 1-37.

[7] Noder, J., Dykeman, J., Butcher, C. (2021). New Methodologies for Fracture Detection of Automotive Steels in Tight Radius Bending: Application to the VDA238-100 V-Bend Test. *Experimental Mechanics* 61, 367-394.

[8] Fast-Irvine, J.C. (2022). Experimental Methods for the Constitutive Characterization of Sheet Materials in Generalized Plane Strain. MASc Thesis. Available online to download.

FOR MORE INFORMATION

Name: Cliff Butcher

Company: University of Waterloo

Email: cbutcher@uwaterloo.ca

Name: Thomas Stoughton

Company: General Motors

Email: thomas.b.stoughton@gm.com

Name: Eric McCarty

Company: Auto-Steel Partnership

Email: emccarty@a-sp.org

More Questions? Meet the speaker(s) at the Auto/Steel Partnership booth.

A/S P Auto/Steel Partnership